Remote sensing of vegetation and land-cover change in Arctic Tundra Ecosystems

Douglas A. Stow[a,*], Allen Hope[a], David McGuire[b], David Verbyla[c], John Gamon[d],
Fred Huemmrich[e], Stan Houston[d], Charles Racine[f], Matthew Sturm[g], Kenneth Tape[h],
Larry Hinzman (Professor of Water Resources)[i], Kenji Yoshikawa[i], Craig Tweedie[j],
Brian Noyle[k], Cherie Silapaswan[l], David Douglas[m], Brad Griffith[n], Gensuo Jia[o],
Howard Epstein[o], Donald Walker[p], Scott Daeschner[a],
Aaron Petersen[a], Liming Zhou[q], Ranga Myneni[r]

[a] Department of Geography, San Diego State University, San Diego, CA 92182-4493, USA
[b] U.S. Geological Survey, Alaska Cooperative Fish and Wildlife Research Unit, University of Alaska Fairbanks, Fairbanks, AK 99775, USA
[c] Department of Forest Sciences, University of Alaska Fairbanks, Fairbanks, AK 99775, USA
[d] Center for Environmental Analysis and Department of Biological Sciences, California State University, Los Angeles,
5151 State University Drive, Los Angeles, CA 90032, USA
[e] Joint Center for Earth Systems Technology (JCET), University of Maryland Baltimore County, Code 923.4, NASA's Goddard Space Flight Center,
Greenbelt, MD 20771, USA
[f] USA CRREL, 72 Lyme Rd., Hanover, NH 03755, USA
[g] USA-CRREL-Alaska, P.O. Box 35170, Ft. Wainwright, Alaska 99703-0170, USA
[h] Geophysical Institute, University of Alaska, Fairbanks, AK 99775, USA
[i] Water and Environmental Research Center, Institute of Northern Engineering, University of Alaska Fairbanks,
P.O. Box 755860, Fairbanks, Alaska 99775-5860, USA
[j] Arctic Ecology Laboratory, Department of Plant Biology, Michigan State University, East Lansing, MI 48824-1031, USA
[k] Space Imaging Solutions, Michigan Office, 455 Eisenhower Parkway, Suite 70, Ann Arbor, MI 48108, USA
[l] Department of Biology and Wildlife, University of Alaska Fairbanks, Fairbanks, AK 99775, USA
[m] USGS Alaska Biological Science Center, Glacier Bay Field Station, Juneau Office, PO Box 240009, Douglas, AK 99824-0009, USA
[n] USGS Alaska Cooperative Fish and Wildlife Research Unit, PO Box 757020, University of Alaska Fairbanks, Fairbanks, AK 99775, USA
[o] Department of Environmental Sciences, University of Virginia, Charlottesville, VA 22904-4123, USA
[p] Institute of Arctic Biology, University of Alaska Fairbanks, Fairbanks, AK 99775-7000, USA
[q] Atmospheric Dynamics and Climate, School of Earth and Atmospheric Sciences, Georgia Institute of Technology, Atlanta, GA 30332-0340, USA
[r] Department of Geography, 675 Commonwealth Avenue, Boston University, Boston, MA 02215, USA

Abstract

The objective of this paper is to review research conducted over the past decade on the application of multi-temporal remote sensing for monitoring changes of Arctic tundra lands. Emphasis is placed on results from the National Science Foundation Land–Air–Ice Interactions (LAII) program and on optical remote sensing techniques. Case studies demonstrate that ground-level sensors on stationary or moving track platforms and wide-swath imaging sensors on polar orbiting satellites are particularly useful for capturing optical remote sensing data at sufficient frequency to study tundra vegetation dynamics and changes for the cloud prone Arctic. Less frequent imaging with high spatial resolution instruments on aircraft and lower orbiting satellites enable more detailed analyses of land cover change and calibration/validation of coarser resolution observations.

The strongest signals of ecosystem change detected thus far appear to correspond to expansion of tundra shrubs and changes in the amount and extent of thaw lakes and ponds. Changes in shrub cover and extent have been documented by modern repeat imaging that matches archived historical aerial photography. NOAA Advanced Very High Resolution Radiometer (AVHRR) time series provide a 20-year

---

* Corresponding author. Tel.: +1-619-594-5498; fax: +1-619-594-4938.
E-mail address: stow@mail.sdsu.edu (D.A. Stow).

record for determining changes in greenness that relates to photosynthetic activity, net primary production, and growing season length. The strong contrast between land materials and surface waters enables changes in lake and pond extent to be readily measured and monitored.

1. Introduction

Arctic ecosystems are characterized by low air and soil temperatures, permafrost, a short growing season, and limited vegetation productivity. These ecosystems are considered to be particularly sensitive to disturbance (Reynolds & Tenhunen, 1996) which is a "change in vegetation or the underlying substrate caused by some external factor" (Walker, 1996, p. 35). These external factors range from localized events, such as energy exploration or lightning induced fires, to global climate change. While the direct effects of human activity in Arctic regions may be localized, the impact of global climate change may have regional consequences.

Predictions of global warming based on General Circulation Models (GCMs) consistently indicate the largest relative warming for northern high latitudes, which includes the Arctic tundra biome (Kattenburg et al., 1996). Substantial changes in precipitation are also expected in Arctic regions (Maxwell, 1992). Meteorological records from Siberia, northwestern Canada and Alaska indicate that these predicted temperature and precipitation changes might already be occurring (Serreze et al., 2000; Williams & Rastetter, 1999).

An increase in Arctic temperatures has the potential to alter vegetation cover in a number of ways. Vegetation production may increase in response to warmer temperatures (Williams, Eugster, Rastetter, McFadden, & Chapin, 2000) and longer growing seasons, as snow depth decreases and snow melts earlier in the spring (Groisman, Karl, & Knight, 1994). Changes in temperature, permafrost depth, soil moisture, water and nutrient fluxes in Arctic regions could alter the competitive advantage of different species and modify ecosystem composition and vegetation cover characteristics (Serreze et al., 2000; Walker et al., in press).

Warming in northern high latitudes over the past three decades has not been uniform across the region (Hansen, Ruedy, Glascoe, & Sato, 1999). Consequently, the impacts of warming on ecosystem processes and the response of vegetation may demonstrate similar spatial variability. There is evidence to indicate that climatically induced changes in vegetation cover and composition need to be monitored at different spatial scales. Local increases in shrub cover in an Arctic tundra ecosystem over a 50-year period have been documented by Sturm, Racine, & Tape (2001). Increases in above-ground production of arctic tundra and boreal forest vegetation have been reported for large regions that lie within 45°N and 70°N (Myneni, Keeling, Tucker, Asrar, & Nemani, 1997; Tucker et al., 2001; Zhou et al., 2001), and positively correlate with atmospheric CO_2 measurements (Keeling, Chin, & Whorf, 1996; Oechel, Vourlitis, Hastings, & Bochkarey, 1995; Randerson, Field, Fung, & Tans, 1999).

Climatically induced changes to ecosystem composition and production may be expected to occur over different temporal scales, although these are not independent processes. Changes in composition may require decades to be discernable, while ecosystem phenology and production characteristically exhibit detectable interannual variability (Arft et al., 1999; Hope, Pence, & Stow, in press; Markon, Fleming, & Binnian, 1995). Of key interest is whether changes in productivity and phenology follow a trend over decadal time scales.

Remote sensing has the potential to detect and monitor changes in Arctic vegetation at a variety of spatial and temporal scales. Ground-level sensors and high spatial resolution imaging systems can be used to monitor selected study sites, to detect changes in vegetation composition or structure and to determine the nature of changes identified from coarser resolution satellite sensors. The frequency of aircraft observations is constrained by logistical difficulties in remote Arctic locations, inclement weather and costs. Furthermore, historical aircraft data sets are unlikely to have been collected according to a regular schedule or to cover large areas. In contrast, satellites can theoretically image large regions on a regular basis. The use of optical remote sensing systems in Arctic regions faces a number of challenges, including frequent cloud cover (Hope et al., in press). Radar systems can collect data regardless of cloud cover conditions, but have a different set of associated problems (e.g., terrain effects and view angle dependencies) that must be overcome to derive useful information on changes in vegetation properties and composition.

The objective of this paper is to synthesize results of research conducted over the past decade on the application of multi-temporal remote sensing for monitoring changes of Arctic tundra lands. Emphasis is placed on results from the National Science Foundation Land−Air−Ice Interactions (LAII) program and on optical remote sensing techniques (LAII, 2001).

The paper begins with an overview of multi-temporal remote sensing and the special challenges and opportunities for land cover change applications in the Arctic. This includes both the signals of land cover change that may be detectable, as well as the noise sources from remote sensing processes that may obscure signals or create arti-

facts. The bulk of the paper consists of a series of case studies of multi-temporal remote sensing research on monitoring of changes of Arctic lands. These scales of these case studies span a range of spatial resolutions from 1 m to 10 km, spatial extents from 100 m to circumpolar, and time durations from months to 20 years.

2. Potential remote sensing signals of vegetation change in arctic ecosystems

Arctic vegetation communities can undergo a variety of changes in response to climate change. Remote sensing has the potential to identify a number of these changes including changes in above ground production, structure and cover, phenological growth characteristics, and ecotones/boundaries. As mentioned previously, changes in a number of these vegetation characteristics can occur simultaneously. For example, an increase in shrub cover in a tussock tundra ecosystem may represent a shift in species composition and/ or abundance, and lead to an increase in net primary production. Using remote sensing to detect changes in vegetation structure and function may require monitoring at contrasting spatial and temporal scales. As with many other remote sensing applications, different remote sensing spatial, temporal, radiometric and spectral resolutions need to be considered to study signals of change in Arctic ecosystems. Furthermore, investigators may need to integrate information from a variety of platforms, and utilize both digital and analog imagery.

Satellite data with high temporal resolution (an overpass at least once a day) have been shown to be particularly valuable for tracking changes in vegetation production at regional, continental and global scales (Goward & Dye, 1987). Consequently, data from the Advanced Very High Resolution Radiometer (AVHRR) and Moderate Resolution Imaging Spectroradiometer (MODIS) sensors on polar orbiting satellites are well suited to this application. Data from the MODIS sensor on the Terra and Aqua satellite have enhanced spatial, radiometric, and spectral capabilities compared to AVHRR. Ready access by scientists to MODIS data and the routine production of standardized derivative products (e.g., leaf area index) are beginning to facilitate a variety of multi-temporal vegetation studies. At this time, AVHRR imagery is particularly valuable for land use/land cover studies at decadal time scales since these data are available from the early 1980s to the present.

Multispectral data are often transformed into a spectral vegetation index (SVI) which is intended to be sensitive to changes in vegetation biophysical quantities (e.g., biomass, LAI) while minimizing the effects of different sensor view angles, illumination conditions and soil/moss background. However, Sellers (1985) has shown that the relationship between these indices and biophysical quantities can vary with vegetation type, season, soil background, and the amount of dead material in the plant canopy. Despite these limitations, the use of SVIs to estimate biophysical quantities has become a standard in remote sensing studies. The alternative approach is to invert a canopy reflectance model to derive the biophysical quantities (e.g., Goel, 1985). These models require substantial ancillary information that is generally not available, outside of heavily instrumented experiments. Most SVIs use the contrast between red and near infrared reflectance of green leaves to be sensitive measures of leaf area index and associated biophysical quantities such as green biomass and absorbed photosynthetically active radiation. Indices generally include a difference or ratio of these two spectral bands and the most common index is the normalized difference vegetation index (NDVI) (Myneni & Asrar, 1994). This index is obtained by dividing the difference between near infrared reflectance and red reflectance by the sum of these two reflectance values.

The NDVI has also been the most widely used SVI in biophysical remote sensing studies for Arctic tundra regions and has been shown to significantly relate to vegetation biophysical properties at field plot (Hope, Kimball, & Stow, 1993; McMichael et al., 1999), ground transect (Shippert, Walker, Auerbach, & Lewis, 1995), and NOAA AVHRR (Vourlitis et al., 2000) scales. The emphasis on NDVI is partly a consequence of this SVI being the preferred index in other ecosystems and because standard AVHRR products providing global coverage are based on the NDVI. The NDVI is generally less sensitive to variations in illumination and soil background conditions than a simple ratio of near infrared to red reflectance (Myneni & Asrar, 1994). Also, the relatively continuous cover and predominant green leaf component of Arctic tundra vegetation may account for its common and successful use in past studies (Stow, Burns, & Hope, 1993).

Maximum value compositing (MVC) is the most common form of NDVI compositing used to produce NDVI time-series data sets with minimal effects from clouds and atmospheric scattering (Eidenshink & Faundeen, 1994; Holben, 1986). Frequent cloud cover in Arctic locations, a 14-day or half-monthly compositing period has been shown by Hope, Boynton, Stow, and Douglas (2003) to produce NDVI images with little apparent bias or contamination due to clouds. A time series of these composited NDVI images is the basis for estimating vegetation production. Seasonally integrated NDVI values (SINDVI) correspond closely to vegetation above ground production (Goward & Dye, 1987).

Data from the AVHRR and MODIS sensors provide a means to characterize changes in the phenological growth characteristics of Arctic vegetation. While changes in the SINDVI may indicate a shift in vegetation production, phenological studies that examine growing season start and end dates (e.g., Zhou et al., 2001) and magnitude of peak "greenness" (e.g., Hope et al., in press; Markon et al., 1995), supported by ground-based validation (Gower, Kucharik, & Norman, 1999), could provide insights into the causes of increased production.

The species mix in Arctic tundra vegetation communities may change in response to disturbances originating at local scales (e.g., human settlement) or global scales (e.g., climate change). Multi-level remote sensing provides a potential means for monitoring large areas on a continuous basis and to characterize areas of apparent change. Satellite data may be used to identify general areas of change by examining NDVI time-series data, while aircraft imagery may be acquired to characterize the vegetation in these areas (Stow et al., 2003).

The initial modification to Arctic vegetation composition under a changing climate may be expected to occur at vegetation boundaries or ecotones (Silapaswan, Verbyla, & McGuire, 2001). Satellite multispectral imagery with ground resolution elements of less than 1 km (e.g., Landsat Thematic Mapper (TM)) can provide suitable data sets for studying vegetation structural changes and ecotone dynamics.

Arctic landscapes are often characterized by a high proportion of lakes or, at certain times of the year, free standing water. Changes in hydrologic fluxes may modify the areal extent and frequency of lakes and the extent or duration of freestanding water. The spectral difference between water and vegetation/soil makes optical remote sensing a potentially effective method to map changes in water bodies. A key consideration in selecting an appropriate data source to monitor changes in Arctic lake cover is the small size of lakes in this region. While high spatial resolution aerial photography and satellite data may be effective for mapping water cover, multi-temporal studies over large regions using these high resolution data are probably not feasible at this time. However, if satellite data are to be used for mapping water cover fractions, including sub-pixel scale water bodies, then a spectral mixture modeling approach will likely have to be employed. Linear mixture modeling with AVHRR data to estimate areal extent of inland water bodies in the North Slope region of northern Alaska (herein called the North Slope) has shown promise (Hope, Coulter, & Stow, 1999). The greater number of spectral bands in MODIS data is likely to make this approach more reliable.

3. Challenges of multi-temporal remote sensing of Arctic tundra ecosystems

While the Arctic tundra biome has or will likely exhibit some of the strongest and earliest signals associated with effects of global change, direct, localized effects from human activities are likely to be limited (Serreze et al., 2000). Capturing signals of land cover change with multi-temporal remote sensing techniques presents a challenge, primarily because of the nature of the Arctic tundra environment. Other technical factors that are not unique to sensing Arctic tundra lands, also add to the complexity of distinguishing signals of global and environmental change.

The longest record lengths of archived remote sensing data are associated with aerial photography (1920s), Landsat Multispectral Scanner (1972 through 2000), and NOAA AVHRR (1982 to present). However, the spatial, spectral, and radiometric fidelity characteristics of these systems are far from optimal. Some ground (Hope et al., 1993; Shippert et al., 1995; Vierling, Deering, & Eck, 1997) and low-level airborne (Stow, Hope, & George, 1993) spectral-radiometric measurements of Arctic tundra vegetation and land cover types have been made, but only recently have multi-temporal observations been conducted with such high spatial resolution (Gammon et al., Section 4.1; Shibayama et al., 1995).

The use of satellite data and SVIs to estimate regional-scale patterns of biophysical quantities requires field measurements of the two variables to establish the basic predictive model. These models are likely to be scale and sensor dependent and their use with data from satellites may incur substantial uncertainty. Furthermore, obtaining samples large enough to represent the spatial heterogeneity of natural ecosystems is challenging given the logistical difficulties of collecting field data in Arctic ecosystems.

Five factors that are mostly unique to Arctic tundra environments limit the effectiveness of multi-temporal optical sensing, particularly from satellites and most aircraft platforms: (1) short growing season length, (2) persistent cloud cover, (3) solar geometry, (4) standing water and shallow lakes, and (5) snow and ice cover (Hope & Stow, 1995).

A short (2 to 4 months) snow-free, summer growing season means that Arctic vegetation has adapted to a short growing season, such that phenological development takes place rapidly. Similarly, surface hydrological processes progress rapidly and hydrological events have short durations. This means that remote observations must be made at high temporal frequency in a relatively short period, in order to capture specific features of these cycles.

Cloud cover of Arctic tundra lands is persistent, particularly during the short summer growing season. Even for large field-of-view, polar orbiting satellite systems (e.g., NOAA AVHRR) that enable multiple acquisitions each day, cloud-free observations may not occur for several weeks at a time. This means that ground or low-level airborne optical sensing under cloud cover may be necessary to capture dynamic processes during the brief summer growing season (Gammon et al., Section 4.1; Hope et al., 1999).

Optical remote sensing of Arctic lands is mostly limited to observations during the relatively short growing season. The solar radiation characteristics of the growing season include very long periods of sunlight and large solar zenith angles. Long day lengths enhance the opportunity to capture optical remotely sensed data, but are accompanied by a large range of solar azimuth and zenith angles. Low incident sun rays mean that shade is an important factor in contributing to the at-sensor solar radiance, even for the characteristically

low stature vegetation and gentle relief of Arctic tundra (McGuffie & Henderson-Sellers, 1986). Solar zenith angles are always greater than 43° and become so large late in the growing season that signal-to-noise ratios drop to a level that precludes useful sensing.

Because permafrost substantially limits the drainage of Arctic tundra soils and evaporation is limited, much of the surface is covered by standing water or shallow thaw lakes. Monitoring the spatial and temporal variability of water cover could be critical to quantifying and understanding regional energy, water, and carbon fluxes (Hinzman et al., Section 4.3; Hope et al., 1999). However, this variability, particularly for standing water cover, may bias estimates of vegetation properties and their dynamics from low spatial, high temporal frequency satellite measurements.

Similar to surface water, variations of snow and ice cover may be signals of interest related to climate variation, or they may mask or bias remote measurements of vegetation properties or processes. For instance, there has been much interest in determining if growing season length has been increasing over the past few decades, by making spatially explicit estimates of the dates of snowmelt and snow accumulation from satellite image data (Myneni et al., 1997; Shabanov, Zhou, Knyazikhin, Myneni, & Tucker, 2002; Stone, Dutton, Harris, & Longenecker, 2002; Tucker et al., 2001). However, high spatial and temporal variability of snow and ice (lake and land) melt over Arctic tundra regions results in varying sub-pixel mixtures with vegetation cover, which may influence bias in the predictive relationship between SVIs and tundra biophysical properties.

Temporal variations in several aspects of the remote sensing process are not necessarily specific to Arctic tundra studies, but can substantially impact the viability of quantitative assessments of changes in tundra biophysical properties. They tend to be less critical when determining changes in land cover type or composition. These time-varying technical factors include changes in: (1) sensor and platform characteristics (Kaufmann et al., 2000; Roa & Chen, 1999; Tahnk & Coakley, 2001; Trishchenko, Cihlar, & Li, 2002), (2) atmospheric and solar effects (Jeyaseelan & Thiruvengadachari, 1993; Hope et al., in press), and (3) sensor view geometry. Most research on these effects primarily pertains to the NOAA AVHRR and to a lesser degree, Landsat MSS and TM systems, because of their longer record lengths.

4. Case studies

Nine case studies are presented that demonstrate the use of multi-temporal remote sensing approaches to monitoring changes of Arctic ecosystems. All of these are based on optical remote sensing of land cover changes, and all but two are based on studies conducted for the North Slope. The case studies are presented in order of decreasing spatial resolution and increasing extent of coverage. Specific authors are listed after the case study title, with affiliations designated on the title page.

4.1. Ground-level multi-temporal spectroscopic analysis of tundra vegetation dynamics (K. Huemmrich, J. Gamon, and S. Houston)

4.1.1. Introduction

Satellite-derived spectral vegetation indices are often used as indicators of snowmelt and potential photosynthetic activity (e.g., Law & Waring, 1994), and have indicated earlier spring snowmelt and increased photosynthetic activity in northern latitude ecosystems in recent years (e.g., Myneni et al., 1997). However, satellite measurements may be confounded by poor visibility, particularly in the North Slope of Alaska where cloud cover frequently obscures the surface. This case study highlights novel methods of monitoring surface optical properties based on near-range remote sensing, thus eliminating the complicating effect of atmospheric interference. These methods are used to reveal remarkable spatial and temporal dynamics in vegetation activity related to photosynthetic carbon flux.

4.1.2. Data and methods

To characterize spatial and temporal patterns of photosynthetic activity, the sampling methods employed periodic optical sampling (spectral reflectance) at multiple spatial scales. A 100-m-long track system was established that allowed a tram cart to carry a spectroradiometer (Unispec DC, PP Systems) along a transect across the tundra. One fiber-optic head of the spectroradiometer was mounted on a tower attached to the cart, allowing the instrument to view an area south of the track with a ground resolution element of approximately 1 m in diameter (Fig. 1). Simultaneously with a measurement of reflected radiance, a measurement of incident radiance was also acquired with a second detector monitoring sky irradiance. The coincident measurement of irradiance and reflected radiance allowed this system to operate under all cloud cover conditions. The tram system minimized disturbance of the tundra surface, while enabling the collection of accurately located measurements.

4.1.3. Results

Significant variability in NDVI was observed at the meter scale along the transect, both for individual days and for seasonal patterns. At the 100 m scale, averaged reflectances for the tram transect produced NDVI values that were very close in value to average NDVI values for 100 m transects collected within a kilometer of the tram. This indicates that the tram data are representative of the local area, which was confirmed by additional independent measurements and aircraft imagery (not shown).

Fig. 2 shows the spatial and temporal detail of this data set. The very low NDVI values at the beginning of the season (day 159) indicate predominant snow cover along the tramline. Some of this spatial variability is due to micro-
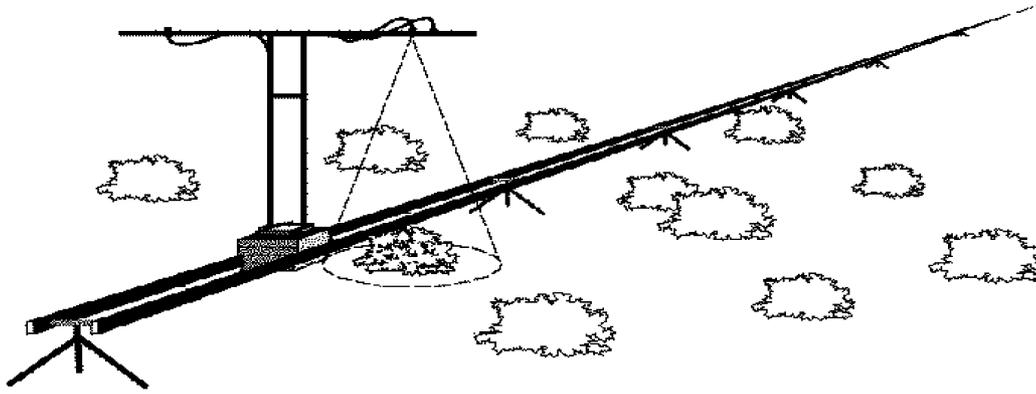
Fig. 1. A graphic display of key elements of the tram system used in the Barrow study. Tracks were leveled and supported above the ground by tripods. A cart ran along the tracks carrying the spectroradiometer. Two fiber-optic heads for the spectroradiometer were mounted on a tower attached to the cart with one head looking upward and the other looking downward at an area next to the tracks. The cart was stopped at every meter along the transect to collect a measurement.

topography. Lower areas tend to be wetter, experience snowmelt later, and have more growth of vascular plants resulting in higher mid-summer NDVI. This NDVI pattern can be observed in Fig. 2 at the 82 m mark, as the tram crosses the trough of a low-centered polygon. On day 159, that location has a negative NDVI, indicating snow cover. On day 169, the snow has melted and the NDVI has increased to 0.32, yet is relatively lower than some surrounding points; but by day 220 this location has become a local maximum with a NDVI of 0.67. Higher polygon areas tend to be well drained and have more lichen and moss cover, resulting in high early season NDVI values but less seasonal change than low-lying patches. This is illustrated in Fig. 2 by the values along a high-centered polygon at the 64 m mark. This location also has a negative NDVI indicating snow cover on day 159. On day 169, NDVI has increased to 0.44, a local maximum. By day 220, it has only increased to

0.54, much lower than the NDVI of the trough at the 82 m mark.

Seasonal differences in regional NDVI were examined at the 100 m scale using NDVI values by averaging reflectances along the total length of the tram transect. Tram average NDVI values for the 2000 and 2001 growing seasons are shown in Fig. 3. In both years, there is a sudden rapid change in NDVI associated with the melting of the snow in mid-June. Through the early summer there is generally a steady increase in NDVI up to a peak around the beginning of August. This peak is then followed by a steady decline in NDVI.

In the 2 years of data collection, there were subtle differences in the NDVI phenologies. Despite a slightly earlier snow, NDVI, and thus, potential photosynthetic activity, showed a delayed development in 2001 relative to 2000, which persisted for the entire season. Consequent-
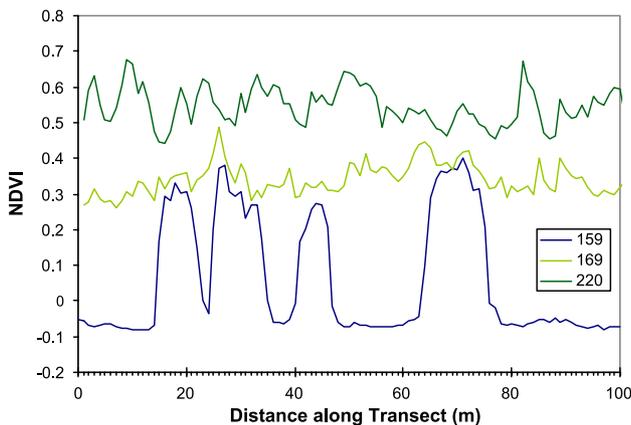

Fig. 2. Optical sampling from the tram system shows the dynamics of NDVI in both time and space. The distance axis is the position along the tram transect, and each line represents the NDVI values measured at every meter along the transect for the day of year of 2001 given in the legend. Day 159 (June 8) was very early in the season, before the snow fully melted, day 169 (June 18) was one of the first completely snow-free days, and day 220 (August 8) was near the seasonal peak growth.
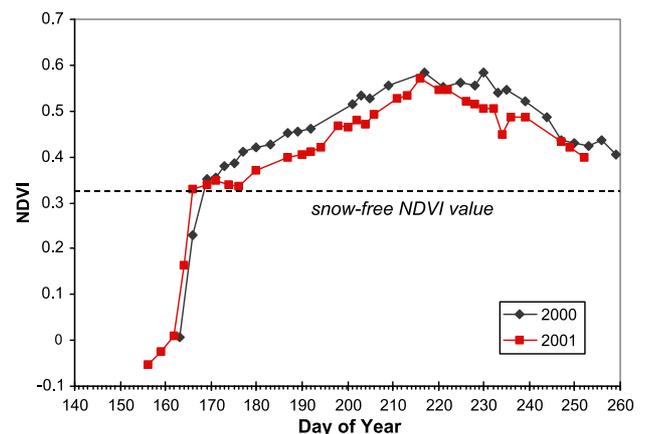

Fig. 3. Seasonal curves of NDVI for transect near Barrow, AK for the 2000 and 2001 growing seasons. Each point is an average of the NDVI of the 100-m-long transect. The curves show sudden increases in NDVI at the beginning of the season due to snow melt, followed by a more gradual increase in NDVI associated with the growth of green plants up to a peak in early August. The latter part of the growing season has a steady decrease in NDVI due to the senescence of the vegetation.

ly, seasonally integrated NDVI (Stow et al., 2003) and thus, the fraction of light absorbed by photosynthetic tissues, was 25% lower in 2001 than in 2000 (indicated by the area above the "snow-free" NDVI value in Fig. 3).

4.1.4. Conclusions

Using a novel remote sensing approach in a wet-sedge tundra ecosystem near Barrow, Alaska, temporal and spatial variability in NDVI was explored for 2000 and 2001. Despite an earlier snowmelt, seasonally integrated NDVI and thus, the fraction of light absorbed by photosynthetic tissues was 25% less in 2001 than in 2000. This reduction in NDVI resulted from early-season cold weather conditions that had a marked impact on whole-season productivity.

Clearly, the dynamics of carbon exchange in this ecosystem can confound simple interpretations based on temporally limited information, such as thaw date or satellite NDVI composites. The data suggest that an earlier start in the growing season does not necessarily lead to enhanced carbon uptake in this northern-latitude ecosystem, which appears to be very responsive to day-to-day weather conditions. These dynamics may not be apparent in satellite measurements that are confounded by cloud cover and limited temporal and spatial resolutions, to resolve day-to-day changes in vegetation growth and photosynthetic activity. The striking intra- and interannual variability in this Arctic tundra ecosystem indicate the importance of *direct* and *continuous* field monitoring to derive and/or validate
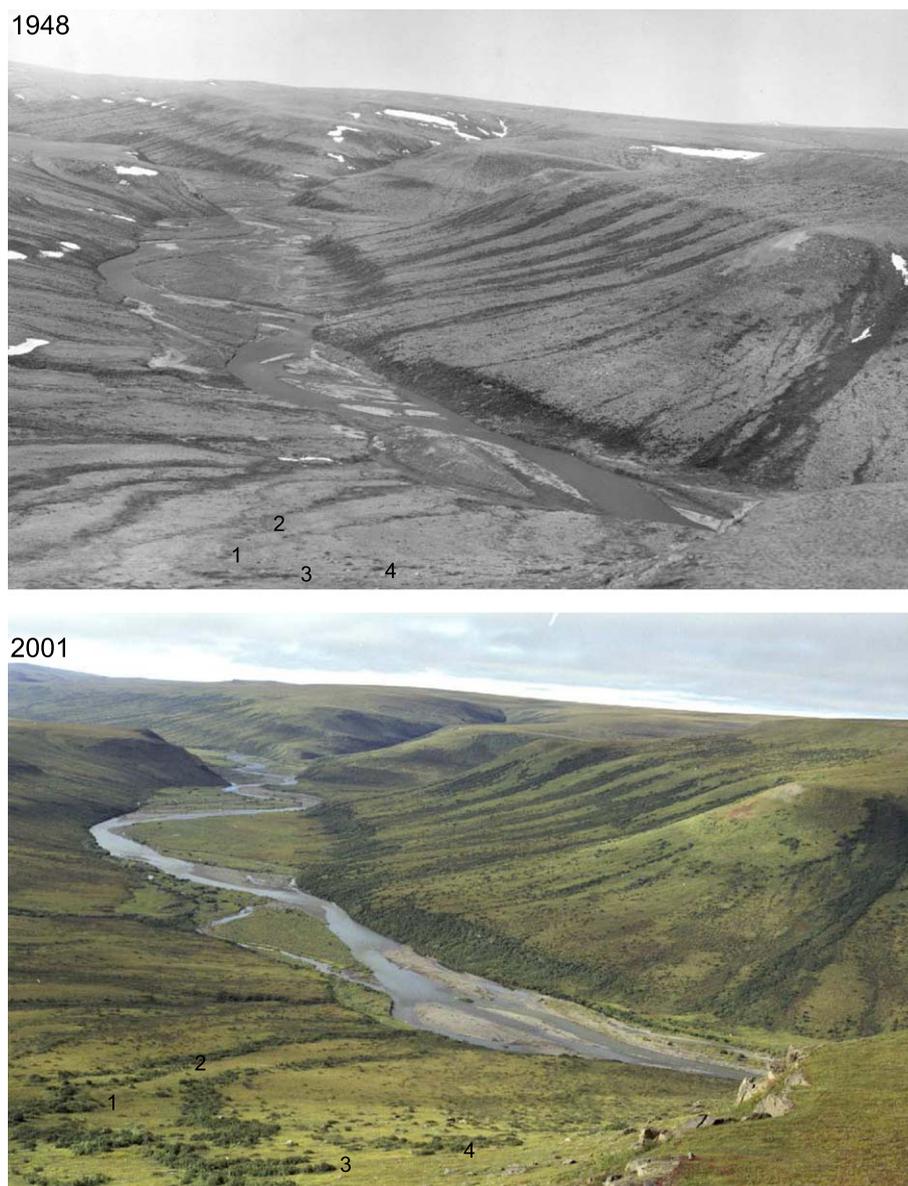

Fig. 4. Original 1948 and 2001 repeat photo of valley slopes along the Chandler River (Photo OV42-17). Increase in the abundance of alder in the foreground is particularly striking. Numbers are provided to match locations on the two photos.

whole-season carbon exchange from temporally limited data (e.g., satellite remote sensing).

4.2. Repeat photography to detect arctic tundra vegetation change during the past half-century (C. Racine, M. Sturm, and K. Tape)

4.2.1. Introduction

The direct comparison of two or more photographs taken at different times from the same location of the same landscape is called 'repeat photography' and has been used in the western United States to assess landscape change over 50 to 100 year time scales (Turner, 1990). Changes in vegetation are subtler in Arctic tundra than in the western US, because of slower rates of change and fewer disturbances related to drought, grazing, and fire. However, the approach may be the best (and sometimes only) way to document changes in vegetation in a region where satellite imagery and direct measurements on plots extend back only about 30 years. The need for these measurements is particularly great because climate warming is expected to produce dramatic changes in the Arctic, including increased shrub growth and northward shifts in tree line (Chapin, Shaver, Giblin, Nadelhoffer, & Laundre, 1995; Lloyd & Fastie, 2002). The generally low stature of tundra vegetation make increases in the height and abundance of shrubs and trees quite apparent on oblique large scale photographs. Tundra

shrub species expected to increase include birch (*Betula nana*), willow (*Salix* sp.) and alder (*Alnus crispa*); tree species which might expand include white spruce (*Picea glauca*) at tree line and the outlier cottonwood (*Populus balsamifera*). Each of these species has a distinct photographic signature.

Arctic vegetation change was evaluated by "repeating" landscape-scale aerial oblique photographs obtained by the U.S. Navy in 1948–1952 (Fig. 4) over a large part of the Arctic Slope of Alaska. These aerial oblique photographs, known as the "COL photographs" (for Colville River), were taken during oil exploration of the Naval Petroleum Reserve (now the National Petroleum Reserve) in Alaska (NPRA). The historical photographs provide a potential record of landscape-scale vegetation change over a broad portion of the Alaskan Arctic during the past half-century coinciding with a period of major climate warming in the Arctic (Lachenbruch & Marshell, 1986).

The COL photographs were taken with a large format (9×18) camera through the open side doors of a twin engine airplane flying 30–200 m above the ground along many of the major and minor river drainages on the Arctic Slope (Fig. 5). The photographic coverage extends a distance of 800 km from east to west (142° to 162°W longitude) and 200 km from tree line on the southwest slope of the Brooks Range (68°N) north to almost 70°N latitude on the Canning River. Over 5000 km of flight lines were photographed to
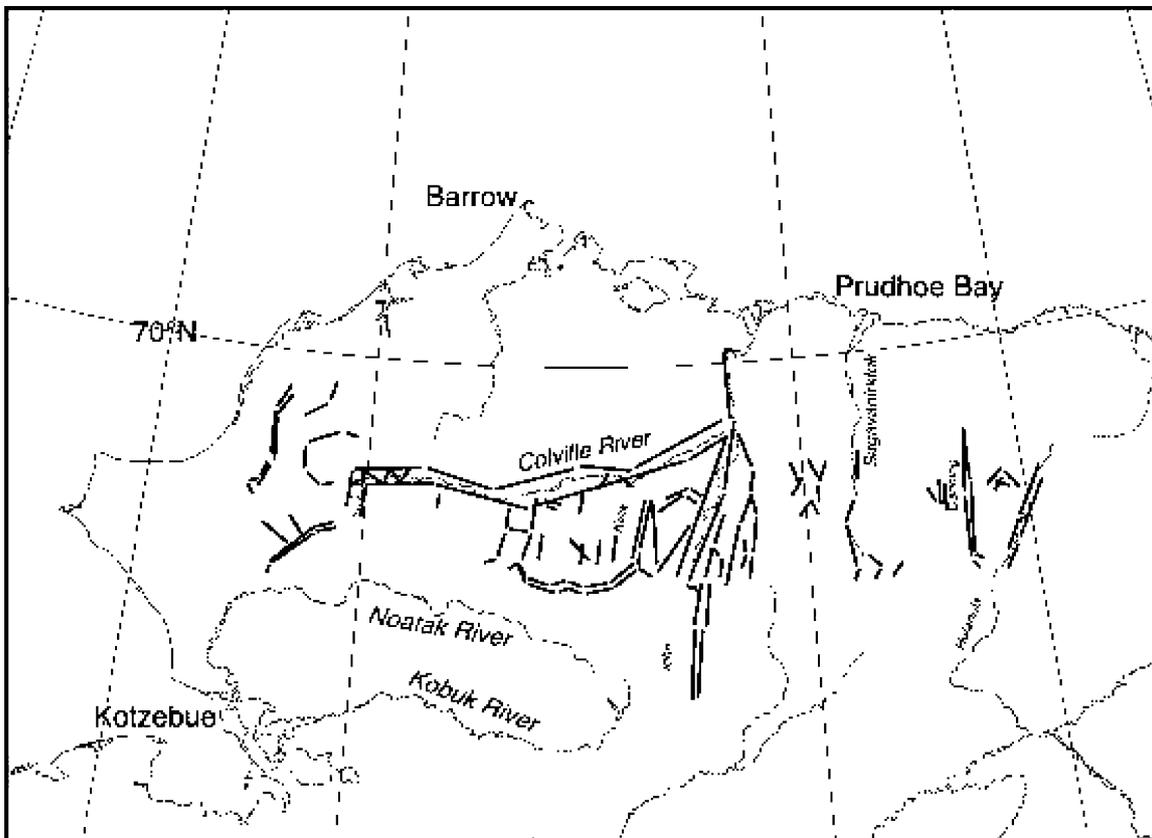

Fig. 5. Map of northern Alaska showing the distribution of COL photo flight lines.

produce a set of more than 6000 low altitude high resolution black and white aerial oblique photographs. Most of the photographs were taken perpendicular to the river and close enough to the ground to provide a good view of vegetation across a toposequence from floodplain and river terraces, to slopes and uplands (Fig. 4). Generally an area in the fore- and middle ground of the photographs covering between 4 and 8 km^2 is clearly visible and useable for comparison.

4.2.2. Data and methods

In order to repeat historical aerial photographs, it was necessary to inventory and select the best ones for use. Many of the old photographs are of poor quality, taken too high above the ground for adequate resolution of shrubs, or cannot be located because of the rudimentary nature of the old flight logs. Based on research in 1999–2001, only about 25% of all of the photographs are suitable for repeating. Even allowing for these unusable photographs, more than 1500 photographs could be repeated profitably. At a rate of about 10 sites per day (avg., 1999–2001growing seasons), about 300 to 400 photographs were repeated during the life of the project that were sufficient for delineating changes in vegetation over a wide area.

Once suitable photographs were chosen, usually in sets of 5 to 20 for a single drainage or flight line, it was necessary to determine the precise location from which each photograph was taken in order to fly back to this position and obtain a second photograph. To accomplish this, a resectioning technique outlined in Moffitt (1970) was implemented. The method requires matching of topographic features on photographs with the same features on 1:63,360 United States Geological Survey (USGS) topographic maps, then using a three-armed protractor to determine the geographic coordinates of the aircraft when the photograph was taken. For each photograph, the computed coordinates were then tabulated and fed into the helicopter GPS. The helicopter was navigated to each photo-point using the GPS, "fine-tuned" position, elevation, and camera pointing angle specifications by visually matching the view to that of the old photograph, and then took multiple pictures using film and digital cameras. Both the original and new film-based copies were scanned at high-resolution.

The new and old photographs were analyzed primarily for changes in the three major deciduous shrubs found in Arctic Alaska, dwarf birch (*B. nana*), willow (*Salix* sp.), and green alder (*A. crispa*). Because of its relatively large size and dark foliage, changes in individuals and stands of alder have been particularly conspicuous and easy to identify. Changes in individual dwarf birch and willow shrubs have not generally been visible on most of the photographs. However, where birch and willow form relatively pure continuous stands, their signature are distinct, enabling changes to be assessed. White spruce, present in the southwestern part of the coverage area, is dark and shows up well on the historical black and white aerial photographs, allowing for confident assessments of changes in tree line.

Table 1 presents a qualitative assessment of change in shrub cover based on careful visual comparison of the photo pairs (old and new) on each flight line. Four change categories were the basis of classification of each image pair: (1) large increase in shrub cover; (2) moderate increase; (3) low or no increase; and (4) decrease in shrub cover. The change classes were combined for each photo pair on a line to derive a magnitude-of-change for each flight line.

In order to give the change assessment a quantitative basis, each photo (old and new) was subsampled using a grid of 10−20 cells of the same size and location on both the new and old photographs. Percent cover of shrubs was estimated for each cell as well as the level of confidence in the assessment. Where an increase in shrub cover was observed, the reason for change was evaluated; i.e., infilling, shrub boundary expansion; shrub size increase, density increase. The areal extent of each cell was estimated so as to extrapolate percent cover increase to change in area and shrub biomass.

4.2.3. Results

During 1999, 2000, 2001, and 2002, a total of 236 photographs were repeated in 23 different drainages covering the entire upland area of the North Slope of Alaska

Table 1
Flight line drainage locations, number of repeat photographic pairs and half-century magnitude of change in shrub cover for repeat photographs acquired between 1999 and 2002 in 23 drainages on the Arctic Slope of Alaska

Location	No. of photographs	Latitude	Longitude	Magnitude of change
Canning R.	9	69.7692	− 146.4040	Low-none
Ivishak River	5	69.3610	− 148.2355	Moderate
Sag. R.-Lupine	2	69.0882	− 148.8037	Moderate
Sag. R.-Sagwon	5	69.4087	− 148.6003	Moderate
Slope Mtn	9	68.7085	− 149.3190	Low-none
Atigun Gorge	9	68.5084	− 149.0852	Moderate
Nanushuk R.-(N)	9	69.1566	− 150.8413	Moderate
Nanushuk R.-(S)	9	68.7483	− 150.5984	Moderate
Chandler R.	21	68.9252	− 151.8742	High
Anaktuvuk R.-(N)	5	69.4368	− 151.1034	Moderate
Anaktuvuk R. (S)	6	69.0562	− 151.0817	Moderate
Castle Mtn	8	68.6050	− 152.8243	Moderate
The Notch	3	68.3912	− 152.8581	Low-none
Ayiyak River	13	68.8887	− 152.5292	High
Colville R.-Umiat	8	69.2942	− 152.4750	High
Upper Killik R	5	68.3404	− 153.9898	Low-none
Oolamnagavik R	13	68.8368	− 154.1820	High
Ivotuk R.	6	68.4730	− 155.5247	Moderate
Colville R.-Middle	11	68.9388	− 155.8689	High
Kurupa R.	11	68.8889	− 155.1632	High
Upper Colville R.	7	68.8731	− 156.6613	Moderate
Upper Nigu R.	15	68.4702	− 156.4476	Moderate
Nimiuktuk R.	17	68.3442	159.9094	High
Utukok R.	5	68.9972	− 161.0635	Low-none
Kougorurok R.	18	68.0868	− 161.6602	High
Kokolik R.	7	69.2840	− 161.5897	Moderate
Total	236			

(Table 1) ranging east to west from −146.40W to −161.66 W latitude, and south to north from 68.09N to 69.77N. On over half of these photographs evidence was found for distinct increases in shrubs, particularly alder, with no evidence of decreasing shrub cover on any repeat pair. The magnitude of change for all photographic pairs from a given flight line or drainage was similar, permitting the assignment of change for each drainage in Table 1. Of the 26 sets of photographs repeated 50 years apart in 23 different drainages, 8 were rated as high magnitude of shrub increase, 13 as moderate and 5 with low-none magnitude of increase in shrubs. On many photo pairs, it was possible to distinguish between individual alders present in 1948 and 'new' alders that had become established during the past 50 years. In addition, an increase in size of individual alders is easily observed.

Shrub expansion (mainly alder) has been greater in drainages south of the Colville River than elsewhere, with the expansion of alder on the Ayiyak and Chandler River drainages quite dramatic, as can be observed in the foreground of the aerial photographs in Fig. 4. On these drainages, the most notable change has been the in-filling of areas where there were only scattered shrubs in 1948–1952. The repeat pairs have also indicated thickening (increased density) in existing stands of white spruce along the Kougar-urok River, a tributary to the Noatak River, as well as the expansion of spruce into areas that were tundra in 1949. This is consistent with other studies (Suarez, Binkley, Kaye, & Stottlemyer, 1999).

Increases in shrub cover based on comparisons of repeat photographs taken 50 years apart could be influenced by comparing 1948 photographs taken early in the summer before leaf-out with a 2000 photo taken later in the summer. However, the historical photographs were taken on many different dates over the course of several summers and change is visible in repeated photographs independent of date. Snow beds are visible in the older photograph in Fig. 4, even though it was obtained relatively late in the summer on July 4, 1948. Differences in animal browsing might also influence change assessment although alder, the main shrub used to date for change detection, is rejected by most browsers.

4.2.4. Conclusions

A method is described for assessing Arctic tundra vegetation change utilizing a large and exceptional collection of high resolution oblique-aerial photographs obtained over 50 years ago on the North Slope of Alaska. This was achieved by obtaining a photograph from the same location and comparing the old and the new photographs. The advantages of the approach to detecting tundra vegetation change over other remote sensing techniques are that it: (1) provides a longer time scale than plot measurements and satellite imagery which extend back only 20 years, (2) provides more detail than can be obtained from satellite imagery, and (3) is a direct measurement not requiring radiometric cor-

rections or detailed processing. More than 236 photographs have been repeated to date, the majority of which show an increase in shrubs, sometimes by a dramatic amount.

4.3. Use of multi-temporal imagery to detect changes in surface hydrology (K. Yoshikawa and L. Hinzman)

4.3.1. Introduction

Extensive documentation exists in the form of testimonials from local residents that a change in ecosystems seems to be occurring in Arctic regions. However, quantifying hydrologic aspects of that change is difficult because no long-term data on soil moisture or runoff exist for this area. To fill that knowledge gap, aerial photographs and IKONOS satellite imagery covering a study area near Council, Alaska, located near the southern end of the Seward Peninsula, were utilized to document long-term changes that have occurred in the areal coverage of lakes and ponds. This analysis enabled a quantitative interpretation of the hydrological response to a changing climate.

The Seward Peninsula is underlain by discontinuous permafrost, although it appears that in the recent past, the study area was predominantly underlain by continuous permafrost. Ice-rich permafrost maintains a relatively low permeability, greatly restricting infiltration of surface water to the subsurface groundwater. Geophysical surveys, including ground penetrating radar (GPR) and direct boring with complementary temperature measurements, reveal that the permafrost is in the process of degrading (thawing with subsequent subsidence of the surface). Extensive thermokarsting (i.e., surface expression of subsidence due to thawing permafrost) is evident throughout the area (Hinzman, Yoshikawa, & Kane, 2001). Examination of historical oblique photographs from circa 1904 and aerial photography from 1950 reveal numerous tundra ponds, some of which are not present today. These ponds are sustained above the permafrost, or are perched, due to the limited internal drainage. As the permafrost thaws, unfrozen channels develop between and below ponds, allowing subsurface drainage to occur throughout the year.

4.3.2. Data and methods

Twenty-four ponds were examined within an area of about 20 km^2 consisting mostly of tussock tundra and flood plain terrain. Most of the tundra surface has buried ice-wedge networks, indicating contemporary ice-rich permafrost. The areas of the selected ponds were determined using a digital number thresholding technique to distinguish water bodies and shorelines.

Pond areas in 2000 were determined using NDVI images derived from IKONOS multispectral imagery having 4 m spatial resolution. Aerial photographs captured in 1950 (black and white film) and 1981 (color infrared film) were scanned at 1200 dots per inch. Geometric corrections of aerial photographs were conducted to minimize first-order sensor and scanner distortions. A brightness threshold

classification technique was applied to the scanned photography and IKONOS NDVI image, to identify water bodies, shorelines, and land surfaces. Some confusion in distinguishing the main water body from shorelines was caused by floating and submerged vegetation. Field topographic surveys provided ground reference data for validating areal extent of some ponds.

4.3.3. Results

The surface area of most ponds (21 of 24 investigated) has consistently decreased between 1950 and 2000 (Fig. 6). The results of field studies indicate that the ponds are shrinking due to an increase in internal drainage following degradation of permafrost. Evidence of a changing climate is apparent from the climatic data available from Nome, Alaska (approximately 140 km west, Fig. 7). A general warming trend has been ongoing with intermittent cooling periods since 1900. A significant drying period occurred between 1950 and 1976; however, this was followed by a pronounced wetter period from 1976 to present. Despite the wetter and cooler period of the recent past, the ponds have continued to decrease in size. There is no evidence to indicate that encroachment of vegetation surrounding the pond could change the water balance, although recruitment of new vegetation on pond edges is following retreat of the water surface. Ground penetrating radar and other geophysical studies have identified taliks (unfrozen zones surrounded by permafrost) directly beneath some of the shrinking ponds. These taliks extend completely through the permafrost and could allow internal drainage of the ponds.

The benefits of and findings from using multi-temporal imagery to detect changes in thermokarst ponds near Council are: (1) pond bathymetry is consistent, with steep edges and flat bottoms (~1.5 m), (2) sedimentation and vegetation growth rates are low, (3) ice-rich permafrost controlled infiltration of surface water, and (4) there is no liquid water input during winter periods. These factors reduced the impact of other biological or climatological processes that may affect pond area.

4.3.4. Conclusions

The vast majority of the ponds in the study area have decreased in size over the last 50 to 100 years. The decrease in pond area was quantified using multi-temporal imagery and verified with field surveys. Geophysical analyses indicate that the cause of the decrease in pond area is due to degradation of permafrost beneath the pond allowing internal drainage throughout the year. This has broad implications to a changing hydrologic regime on the Seward Peninsula. It also has more immediate and local consequences for migrating waterfowl and other fauna such as caribou. These results demonstrate the value of retrieving and utilizing historical imagery to detect impacts of a changing climate in areas where periodic observations or measurements do not exist. These images may enable further qualitative analysis on such processes as soil moisture dynamics using vegetation and standing water distributions.
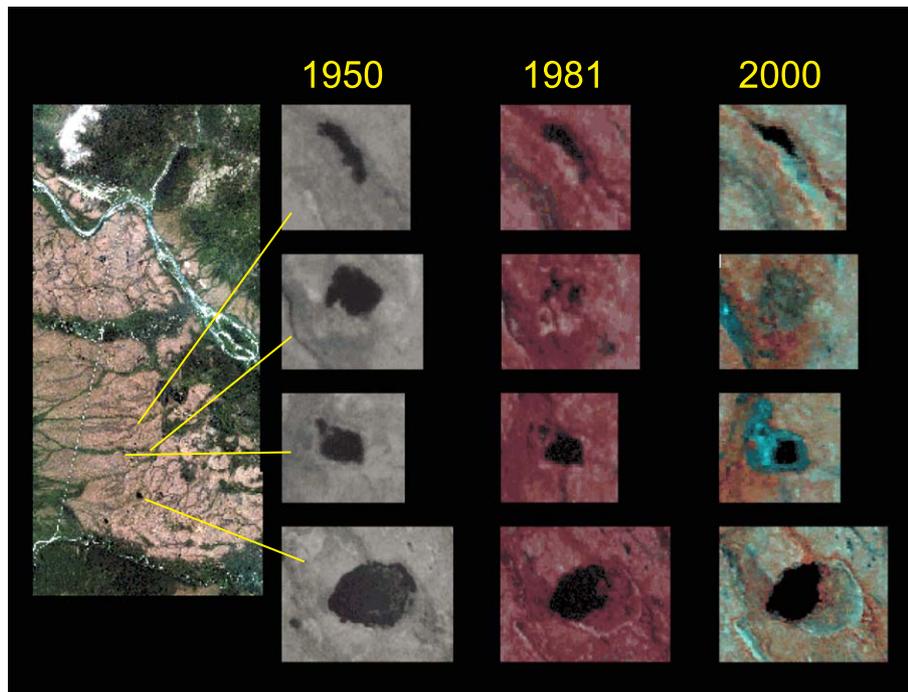

Fig. 6. Multi-temporal analysis of tundra ponds near Council, Alaska utilizing black and white aerial photography, color IR aerial photography and IKONOS imagery.
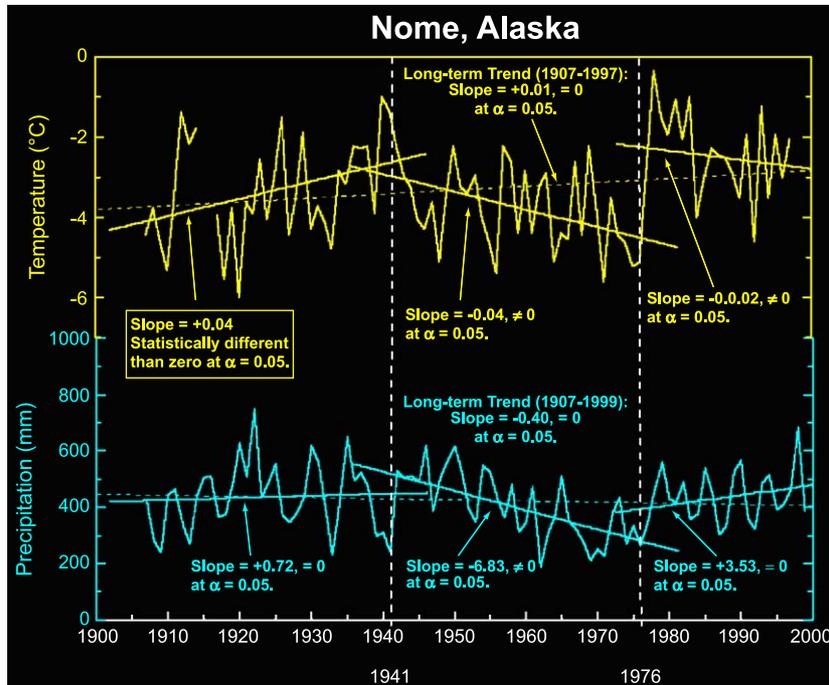
Fig. 7. Long-term trends in air temperature and precipitation collected at the Nome Alaska airport. The data indicate a generalized long-term warming trend with a cooling period between 1941 and 1976. Precipitation has less distinct trends, but dried somewhat between 1941 and 1976, becoming wetter after 1976.

4.4. Potential of IKONOS imagery for arctic land cover change analysis (C. Tweedie and B. Noyle)

4.4.1. Introduction

Few studies have examined changes in Arctic land cover at the landscape level, over decadal time scales (Forbes, Ebersole, & Standberg, 2001; Sturm, Racine, & Tape, 2001). The primary factors limiting analyses of land cover changes in Arctic regions at decadal time scale are the expensive and time consuming nature of aerial photographic approaches when spanning large areas, and the relatively coarse spatial resolution of most satellite sensors (Noyle, 1999). Coarse resolution observations are insufficient for resolving the patch-scale mosaic of the spatially and functionally heterogeneous tundra landscape, especially in coastal plain regions that have significant coverage of patterned ground. Several studies have shown that image classifications of tundra regions that classification accuracies commonly fall below levels achieved for other biomes (Noyle, 1999). New commercial satellites systems having high spatial resolution are available to acquire multispectral imagery of Arctic tundra regions. One of these is the Space Imaging IKONOS satellite, which provides 1 m panchromatic and 4 m multispectral imagery (Donoghue, 2000).

This case study describes the generation of a land cover classification product based on IKONOS satellite imagery for the 3153 ha Barrow Environmental Observatory (BEO), on the North Slope of Alaska and assesses the potential use of this product in combination with archived black and white aerial photography acquired in 1964 to assess patch-scale land cover change over decadal time scales. The

IKONOS classification illustrates the potential use of high spatial resolution satellite imagery and supervised classification methods for mapping of land cover within spatially heterogeneous ecosystems such as Arctic tundra.

4.4.2. Data and methods

Panchromatic and multispectral imagery were acquired for different portions of the BEO at the first snow free period following the launch of the IKONOS satellite (in October 1999), on July 16 and August 16, 2000. Imagery was pan-sharpened using a principle components merge of the four multispectral bands and the panchromatic image, with the resulting image having the spectral characteristics of both inputs and the higher spatial resolution of the panchromatic band. Scenes from acquisition dates were geo-rectified based on ground control points (GCPs) surveyed with a Differential Global Positioning System (DGPS). Imagery from both acquisition dates contained significant ($>20\%$) cirrus cloud cover. Following cloud masking, images from both acquisition dates were mosaicked to minimize cloud cover and were radiometrically balanced. An NDVI image was derived and appended to the mosaic to generate a five-band layer stack in preparation for image classification.

Decision rules for a 15 category hierarchical classification were developed from three former ground-based land cover classification schemes used in the Barrow area by Brown, Everett, Webber, Maclean, and Murray (1980), Walker (1977), and Viereck, Dryness, Batten, and Wenzlick (1992), in concordance with recent plot based vegetation sampling and classification. This classification scheme was

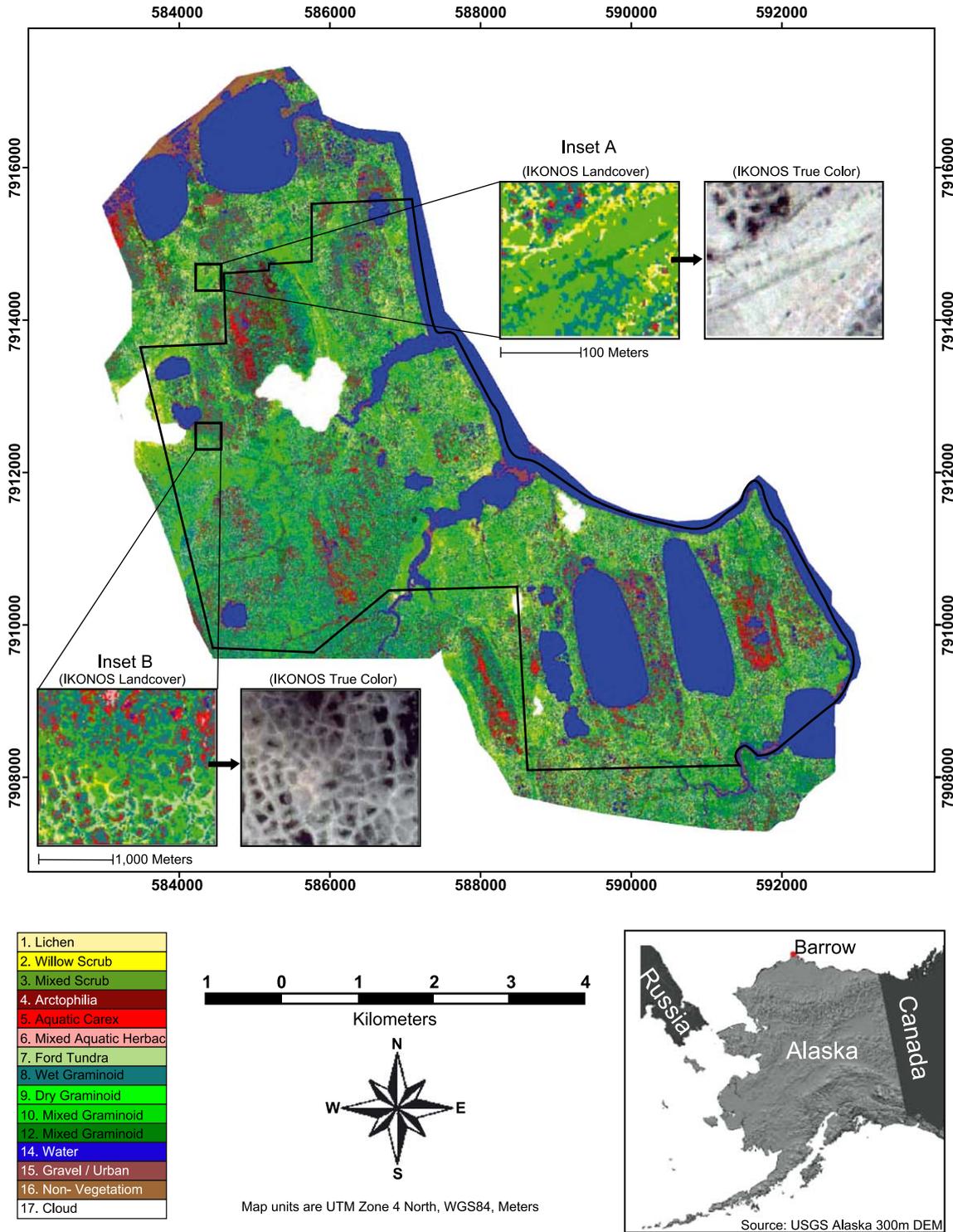## Barrow Environmental Observatory IKONOS Based Land Cover Classification

Fig. 8. Land cover classification derived from IKONOS imagery for the BEO. Inset A and inset B show detailed views of the land cover classification next to the pan-sharpened multispectral IKONOS image, highlighting tracks from off-road vehicle disturbance in the 1960s and polygonized tundra, respectively.

used to select 229 training sites, which formed the basis for supervised classification of the five-band image stack. Agglomerative hierarchical clustering was used to identify outliers, which were removed, resulting in 197 training sites.

Cloud cover and water were identified in an unsupervised classification of the image stack and removed from the image. A supervised classification was performed on the remainder of the image. Initially, only pixels within one

standard deviation of the training site signatures were classified using a parallelepiped rule. The remaining pixels were then classified using maximum likelihood or unlimited spectral distance decision rules.

4.4.3. Results

The resulting classification product is based on a hierarchical classification system with seven major and 15 minor classes. Fig. 8 portrays the classification product derived from IKONOS imagery for the BEO (total area—3153 ha). The extreme spatial heterogeneity detected by the BEO classification product illustrates the utility of IKONOS imagery for detailed assessments of land cover at the landscape scale, based on decision rules developed from ground-based, plot-scale land cover classification of species associations.

An illustration of the spatial detail of the IKONOS classification includes scars left by off-road vehicle use in the 1950s (inset A in Fig. 8), and the various land cover types associated with polygonized tundra (inset B in Fig. 8), demonstrating the utility of this imagery for land management, and the potential for spatial-temporal monitoring of patch-scale land cover dynamics over time. The high spatial resolution of IKONOS panchromatic imagery is comparable to early black and white aerial photography (Fig. 9) in the Barrow region. This highlights the strong potential for conducting land cover change assessments based on comparison of historical aerial photographic and current, high spatial resolution satellite data.

4.4.4. Conclusions

Although an accuracy assessment of the classification described above is currently underway and remains to be completed, this case study has demonstrated the 'coming of age' of multispectral high-resolution satellite imagery and the potential utility of space-borne systems for generating high spatial resolution data on Arctic land cover and land cover change. Such systems are unlikely to replace Landsat TM imagery, due to the higher cost and limited extent of coverage per image frame. However, the utility of this imagery for enhancing land management, long-term land cover monitoring studies, disturbance ecology analyses, and retrogressive land cover assessments is clear. Such high spatial resolution imagery also enables monitoring of land cover change derived from multi-temporal analyses of lower resolution imagery. However, monitoring based on detailed species association based classifications is necessary to support land cover change assessments and further understanding of functional mechanisms associated with and/or driving changes detected using satellite systems.

4.5. Vegetation change on the Seward Peninsula, Alaska (D. Verbyla, D. McGuire, C. Silapaswan)

4.5.1. Introduction

Transects placed along climate gradients have documented shrub tundra replacing tussock tundra in areas of warming climate (Bliss & Matveyeva, 1992). Experimental warming of shrub tundra plots also suggests increased leaf area of existing shrubs (Arft et al., 1999; Bret-Harte et al., 2001; Chapin & Shaver, 1996; Hobbie & Chapin, 1998). Much of the landscape on the Seward Peninsula is in a transition zone between boreal forest and tundra land cover types. Recent climate warming may be an important factor in influencing vegetation cover changes on the Seward Peninsula (Lloyd, Rupp, Fastie, & Starfield, in press).

The potential of using multi-temporal Landsat TM data to detect land cover changes in this area was investigated, with an emphasis on detecting changes in shrub tundra resulting from changes in shrub leaf area and invasion of shrub tundra into tussock tundra. Such changes in Arctic
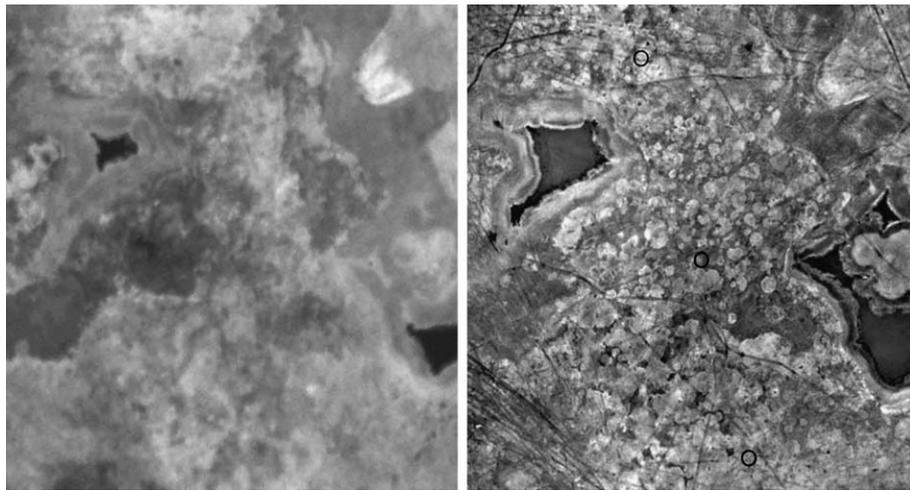

Fig. 9. 2000 IKONOS panchromatic image (left) and 1964 black and white aerial photograph (right, scanned at 1200 dpi, right) of the same locality in Central Marsh on the BEO, illustrating the comparable spatial resolution of these imagery. Note the significant land cover change between 1964 and 2000, including the reduction in coverage of open water in ponds and the apparent recovery of off-road vehicle disturbance in the lower right portion of the image.

shrub communities have been documented elsewhere in Alaska, using historical ground-based and aerial photography (see Section 4.2).

4.5.2. Data and methods

Change vector analysis (Malila, 1980; Johnson & Kasischke, 1998) was applied to multi-temporal Landsat TM data captured in the growing seasons of 1986 (June 29) and 1992 (June 6) and to investigate land cover change on the Seward Peninsula (Fig. 10). Images were co-registered with sub-pixel RMS errors using an affine transformation and nearest neighbor resampling. Radiometric rectification (Hall, Strebel, Nickeson, & Goetz, 1991) was used to normalize each multi-temporal band. Two indices were used as inputs for change vector analysis. The TM4/TM3 (near infrared/red) ratio was used as an index of leaf area (Nemani & Running, 1997; Spanner, Pierce, Peterson, & Running, 1990) and the TM5 band was used as an index of canopy crown shading (Nemani, Pierce, Band, & Running, 1993).

4.5.3. Results

From 1986 to 1992, significant changes in change vectors occurred for covered by the two Landsat TM scenes (Silapaswan et al., 2001), as seen in Fig. 11. In the 1986 image, over 135,000 ha had significant change, primarily as increases in the TM4/TM3 and TM5 indices. There were also areas of significant decrease in the two indices, some of which occurred in two large 1990 burns. The 1992 image had over 110,000 ha of significant change, primarily as a decrease in the two indices. A post-classification change detection, based on unsupervised classification of the 1986

and 1992 TM images indicated the predominant land-cover change to be in the direction of increased shrub cover.

Since increases in leaf area and spatial extent of shrub tundra was of primary interest, areas that had an increase in the TM4/TM3 ratio were investigated. Manual interpretation of aerial photography acquired in 1985 and 1992 was used to identify types of land cover changes that had occurred in these areas. Changes were primarily increases in riparian shrub extent, and density and advance of shrub tundra into tussock tundra in the broad valleys in the northern part of the study area.

4.5.4. Conclusions

This case study indicates that shrub cover on the Seward Peninsula increased in the late 1980s and that tundra is changing predominantly in the direction of increased shrubbiness. Increasing shrub cover is an important result, as it suggests that directional changes are occurring on the Seward Peninsula that are consistent with experimental tundra warming (Chapin et al., 1995). Future remote sensing studies of change using the techniques of this case study can be strengthened with the analysis of images using phenological anniversary dates, since differences between images would be due less to differences in season and vegetation phenology. Future studies should also focus on the extent and location of shrub changes on the Seward Peninsula. Satellite imagery with finer resolution may also help pinpoint areas of potential spruce movement, which were not detectable in this study, even though tree line advance has been measured in ground-based studies (Lloyd et al., in press).
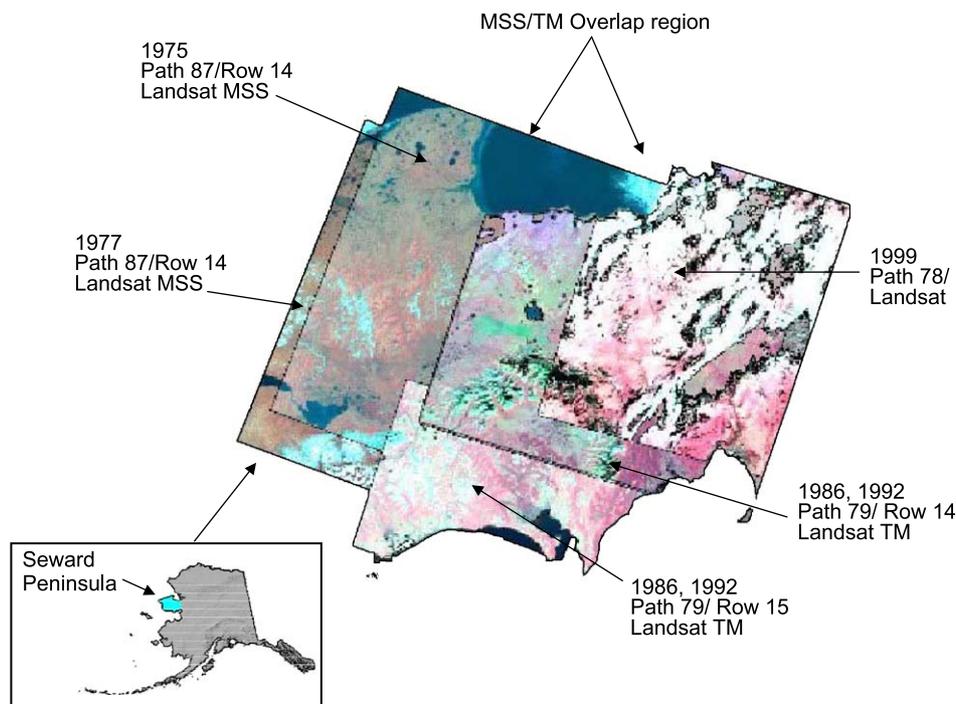

Fig. 10. Location of all acquired Landsat TM and MSS scenes for the Seward Peninsula.
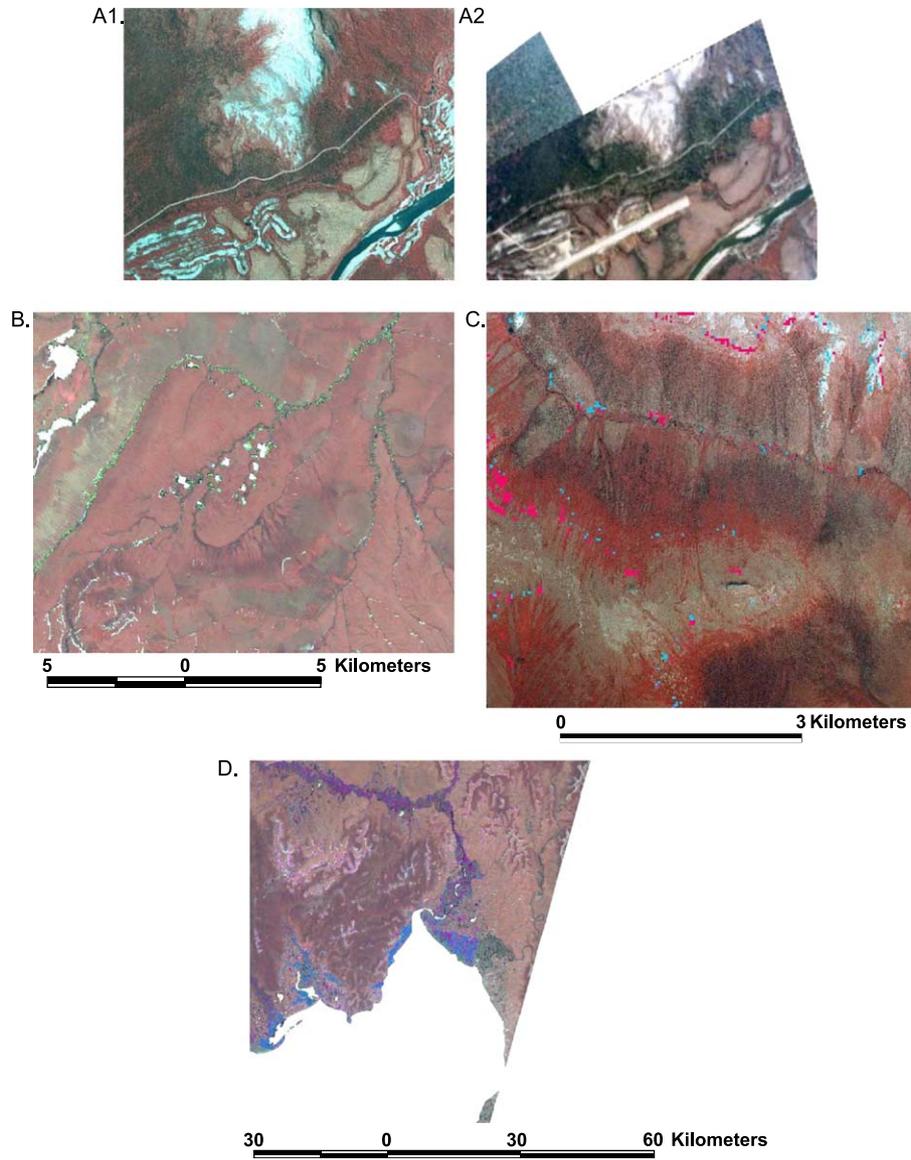
Fig. 11. A1 and A2 are aerial photographs near Council, AK, taken in June 29, 1986 and June 6, 1992, respectively. Forested and shrub vegetation north of the airstrip appears to have increased from 1985 to 1999. (B) Green areas are 1986–1992 CVA results overlaid on a TM image, showing regions of potential increases in TM Band 4/TM Band 3 and decrease in TM Band 5. These changes suggest that shrubs have increased along riverbeds. (C) Pink and blue regions are 1986–1992 CVA results overlaid on an infrared aerial photograph, showing areas of detected increases in TM Band 4/TM Band 3 and TM Band 5 (pink), and increases in TM Band 4/TM Band 3 and decreases in TM Band 5 (blue), suggesting an increase in shrub advance. Compared to aerial photograph visual interpretation, shrub advance is approximately 100 m in valleys north of the Bendeleben Mountains. (D) Example of 1986–1992 CVA results greater than the threshold for the Koyuk River Inlet, overlaid on a TM image. Blue areas may represent regions of increases in TM Band 4/TM Band 3 and TM Band 5. Purple areas represent regions of increases in TM Band 4/TM Band 3 and decreases in TM Band 5.

4.6. Documenting annual habitat conditions on caribou calving grounds using AVHRR satellite imagery (D. C. Douglas and B. Griffith)

4.6.1. Introduction

Climate strongly influences the availability and quality of wildlife habitats in Arctic regions. Most wildlife species have adapted seasonal migratory behaviors, synchronized to exploit the Arctic environment during periods optimal to their survival and reproduction. Barren-ground caribou (*Rangifer tarandus*), the longest-distance terrestrial migrants of the northern hemisphere, travel hundreds of kilometers northward every spring (Fancy, Pank, Whitten, & Regelin, 1989) to utilize tundra habitats during the short and highly productive Arctic summer. While timing of calving is relatively constant, environmental conditions vary considerably in concert with annual climate variations. This case study summarizes an investigation of relationships between spring habitat conditions, calving distributions, and calf survival of the Porcupine caribou herd (PCH) in northeast Alaska and the northwest Canada (Fig. 12). Details of this study were originally published in Griffith et al. (2002).
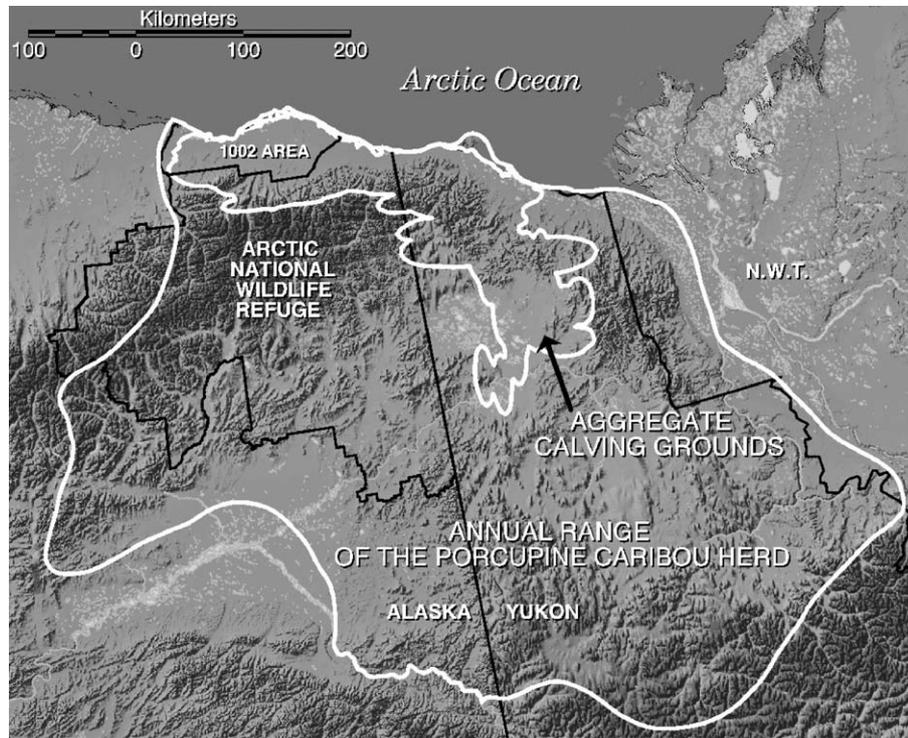
Fig. 12. Total range of the Porcupine caribou herd and the aggregate extent of all annual calving grounds, 1983–2001, northwest Alaska and northeast Canada.

4.6.2. Data and methods

Documenting historic patterns of annual snow distribution and vegetation phenology on the calving grounds of the PCH is well suited to the daily digital archives of AVHRR data. Full-resolution AVHRR images of the study area were acquired during late-May through early-July, 1985–2001. The visible and near-infrared AVHRR channels were calibrated to account for post-launch sensor degradation of the NOAA-9 and NOAA-11 (Teillet & Holben, 1994), NOAA-10 and NOAA-12 (Loeb, 1997), and NOAA-14 (Mitchell, 1999) instruments.

Maximum NDVI (Tucker, 1979) composite images (Holben, 1986) were derived over short chronological periods (mean 5.3 days, S.D.=2.6 days) to minimize cloud contamination but maintain temporal specificity. Remaining cloudy pixels were identified and removed from analysis when AHVRR channel-3 minus channel-4 exceeded 12 K (Baglio & Holroyd, 1989). AVHRR pixels were also excluded if their associated satellite zenith angle exceeded $50°$ or their solar zenith angle exceeded $75°$. Morning and afternoon AVHRR satellite data were pooled to maximize viewing opportunities within the short composite periods. Pooling morning and afternoon passes likely introduced an unbiased source of noise among the NDVI composites due to the influences of diurnally dependent solar and satellite geometries (Kaufmann et al., 2000; Privette, Fowler, Wick, Baldwin, & Emery, 1995).

Three maximum NDVI composite images were produced for each year: (1) peak calving (NDVI_calving, mean image date of June 2, SE=2.0 days), (2) mid-June (mean image date of June 16, SE=2.6 days), and (3) early July (mean image date of July 3, SE=2.4 days). A pixel-based daily rate of NDVI increase between the calving and mid-June composites was calculated (NDVI_rate), and NDVI on 21 June was linearly interpolated from the mid-June and early-July composites (NDVI_621).

The annual medians of NDVI_calving and NDVI_621 were assumed to represent the quantity of green forage that was available to caribou, while NDVI_rate was assumed to represent forage quality, because it estimated accumulation of new plant tissue, which is highly digestible (Cameron & Whitten, 1980). The quality implication of NDVI_rate was based on the assumption that caribou forage selectively for the most digestible food items (White, 1983). Because milk intake by caribou calves remains high during the first 3 weeks of life, then declines as the calves increase their intake of vegetation (Parker, White, Gillingham, & Holleman, 1990; White & Luick, 1984), NDVI_621 was assumed to represent an integrated measure of forage that was available to cows during their energetically demanding 3-week period of peak lactation.

Annual calving grounds (ACG) of the PCH, and the annual concentrated calving areas (CCA) within each ACG were defined by fixed kernel analyses of radio-tracking locations (annual mean n=40, se=18) collected by Federal, State, and Canadian biologists. The aggregate outer boundary of all ACGs, 1983–2001, encompassed a 36,000 km^2 area, and defined the total extent of calving (Fig. 12).

4.6.3. Results

Annual selection of calving habitats by the PCH was found to be scale-dependent. Within the total aggregate extent of calving (broad-scale), females selected annual calving grounds with proportionately greater area of high (>median) NDVI_rate ($P=0.005$), proportionately less area with high NDVI_calving ($P=0.001$), and proportionately less area with high NDVI_621 ($P=0.002$). In contrast, PCH females selected concentrated calving areas within the annual calving grounds (local scale) that had proportionately greater area of high NDVI_calving ($P=0.002$) and proportionately greater area of high NDVI_621 ($P<0.001$). In other words, PCH females selected annual calving grounds with a high proportion of easily digestible forage (NDVI_rate), and then locally selected concentrated calving areas (within the ACG) with relatively high plant biomass at calving and on June 21 (NDVI_calving, NDVI_621). Thus, there appears to be a scale dependency in the selection of forage quantity and quality. The basis of habitat selection shifted from forage quality (NDVI_rate) to forage quantity (NDVI_calving, NDVI_621) between the two scales.

Within the aggregate extent of calving, the amount of forage available to cows at peak lactation (NDVI_621) provided the best model of calf survival during June ($r^2=0.85$, $P < 0.001$; Fig. 13). No other independent variable that was considered added significant explanatory power. At local scales within just the annual calving grounds, the proportion of PCH calves that survived through June was positively related to both NDVI_621 and to the proportion of calves that were born on the coastal plain ($r^2=0.70$, $P<0.001$), an area of putatively reduced predation risk (Griffith et al., 2002).

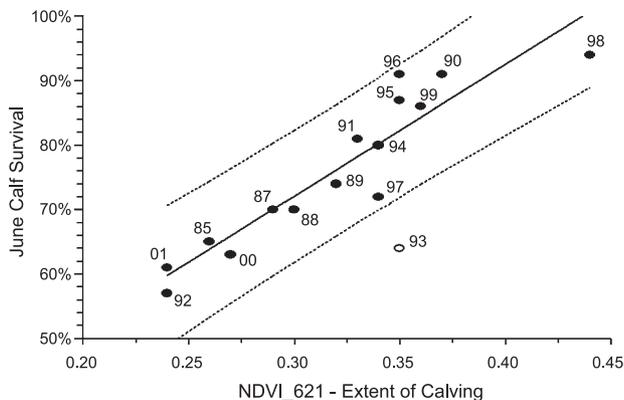Fig. 13. Percent June calf survival for the Porcupine caribou herd, 1985–2001, in relation to median NDVI on June 21 (NDVI_621) within the aggregate extent of calving (Percent June Calf Survival=[0.107+ (2.05×NDVI_621 in the extent of calving)]×100). Legends identify the year of the estimate. Calf survival was not estimated in 1986 because inclement weather prevented a near-complete sample in late June. Calf survival for 1993 was a significant outlier ($R_{Student}=3.84$) and excluded from the estimated regression line ($r^2=0.85$, $P<0.0001$). Upper and lower dashed lines indicate 95% confidence intervals on the predicted observations (from Griffith et al., 2002).

4.6.4. Conclusions

The timing of snowmelt and vegetation phenology within the PCH calving range influenced the annual selection of calving areas, and was correlated with the survival of calves during June. Calving females selected areas with high vegetation growth rates (quality) at broad scales, and then locally selected areas with high vegetation biomass (quantity). Spring arrival on the calving ground is the time of minimum body reserves for parturient females (Chan-McLeod, White, & Holleman, 1994; Chan-McLeod, White, & Russell, 1999). Thereafter, their energy and protein requirements reach the highest level of the year during peak lactation in the first 3 weeks of June (Parker et al., 1990; White & Luick, 1984). The females, appetites are high and forage intake rates can match lactation demand only where primary production is high (White et al., 1975; White, Bunnell, Gaare, Skogland, & Hubert, 1981). Small changes in nutritional content and digestibility of forages, however, can have substantial multiplier effects on digestible energy and protein intake (White, 1983), and thus may influence nutritional performance of PCH females on the calving ground, and the subsequent survival of their calves. During years with more advanced vegetation phenology, the PCH tended to select calving areas on the coastal plain, where abundant digestible forage and putatively low predator densities both may have contributed to high June calf survival rates.

Earlier vegetation greening and later senescence have been detected with NDVI time series for the Northern Hemisphere (north of 40°N), (Myneni et al., 1997; Zhou et al., 2001), and appear to be associated with an Arctic warming trend during 1990s (Chapman & Walsh, 1993; Groisman et al., 1994; Houghton et al., 1996). Commensurate with the Northern Hemisphere's earlier greening, NDVI_621 also increased linearly within the PCH calving range during 1985–1999 ($r^2=0.496$, $P=0.002$). However, 2000 and 2001 had exceptionally late springs, low NDVI_621, and low June calf survival. Both years were statistical outliers to the increasing NDVI_621 trend of 1985–1999 ($R_{Student}= -2.49$, -2.86, respectively). Future monitoring will be necessary to determine if 2000 and 2001 represent anomalies to, or a departure from, the apparent "warming and greening trends" of the 1990s.

4.7. Climate controls over seasonal dynamics of AVHRR-NDVI for the Alaskan tundra (G. Jia, H. Epstein, and D. Walker)

4.7.1. Introduction

Intra-seasonal patterns of plant growth can be studied to understand vegetation dynamics relative to lower atmosphere dynamics and are therefore, important in evaluating response to climate change (Hope et al., 2003). In Arctic Alaska, vegetation is characterized by strong intra-seasonal dynamic, and vegetation phenology is spatially heterogeneous.

In this case study, intra-annual dynamics of vegetation along several transects in northern Alaska were investigated using a 1995 to 1999 time series of standard biweekly AVHRR NDVI products generated by the USGS. These data were produced using seasonally truncated and composited NDVI images derived from AVHRR Local Area Coverage (LAC) (nominal 1 km spatial resolution) imagery (Jia, Epstein, & Walker, 2002; Jia, Epstein, & Walker, in press). Here, differences in phenology were investigated for various spatial gradients and the effects of climate on such intra-annual patterns.

4.7.2. Data and methods

Multi-year mean NDVI values were calculated for each biweekly compositing period during the 1995 through 1999 growing season. Cloud-contaminated pixels were excluded from the calculation. Four NDVI-based indices were calculated: (1) annual peak NDVI (peak-NDVI, the maximum NDVI value within a year), (2) seasonally integrated NDVI (SINDVI, cumulative NDVI values over 0.09 in a year), (3) onset time of greenness and, (4) length of growing season. Date of onset of greenness indicates when spring foliage becomes dense enough to be detected from background conditions (typically snow). Onset was determined by a threshold NDVI value of ≥ 0.09. Length of growing season is the number of days from onset to senescence in the fall. A threshold of ≤ 0.09 was used for senescence.

Based on a land cover map derived from satellite image analysis (Muller, Racoviteanu, & Walker, 1999) and on aerial photographs, a set of homogenous vegetation patches was selected and geographically referenced, that represented five major tundra types: (1) shrub tundra, (2) moist acidic tundra (MAT), (3) moist nonacidic tundra (MNT), (4) sandy tundra, and (5) wet tundra. Most of the patches selected

were 9 km^2 and were located within homogenous tundra patches. NDVI values of were summarized for three spatial gradients: (1) western North Slope transect, (2) an eastern North Slope transect, and (3) the boundary between acidic and nonacidic tundra.

Regressions between biweekly series of NDVI anomalies vs. mean air temperature (Hinzman, 2001) anomalies were analyzed separately for MAT and MNT around seven sites along the transects. The regressions were performed for Barrow on the western transect, Prudhoe Bay, Franklin Bluffs, Sagwon, and Toolik Lake along the eastern transect, and Umiat and West Kuparuk which are located between the two transects. In an attempt to minimize solar irradiance as a factor that is strongly correlated with both NDVI and temperature, the anomalies from the means were regressed against each other.

4.7.3. Results

Intra-seasonal patterns of NDVI differed amongst vegetation types, as shown in Fig. 14. Wet tundra had the lowest NDVI values for each period, while shrub tundra had the highest values. Peak NDVI occurred in the July 22 to August 4 period for all five vegetation types, with the values of 0.552 for shrub tundra, 0.495 for MAT, 0.436 for sandy tundra, 0.426 for MNT, and 0.343 for wet tundra. The earliest onset of greenness occurs in shrub tundra, followed by MAT, MNT, sandy tundra, and wet tundra. The spatial variation for wet tundra and sandy tundra are greater than other types, which may be indicative of water bodies within wet tundra, and soil parent material and lichen patches varying within sandy tundra (Walker et al., 2003).

The spectral-temporal profiles of NDVI values also portray the difference between phenological patterns among tundra types. Wet tundra and MNT are graminoid or moss-
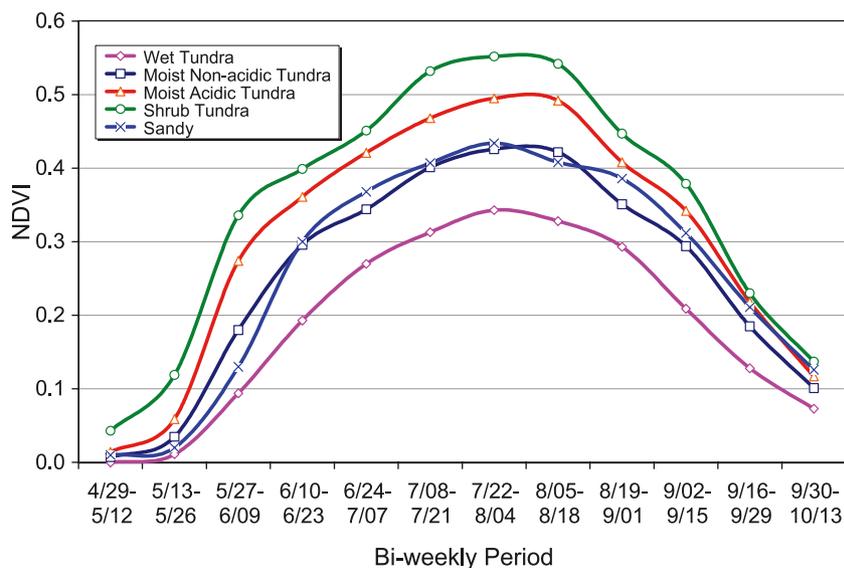

Fig. 14. Intra-seasonal patterns of NDVI among tundra vegetation types. The values are based on 1995–1999 averages, summarized from the homogenous tundra sample sites. Note that periods 1 and 2 occur prior to 4/29 and are not presented on this graph.

dominated plant communities that exhibited relatively smooth and flat intra-seasonal NDVI curves. By contrast, the shrub-dominated tundra exhibited much steeper increases during early growing season, especially in late May, while shrub tundra tends to reach peak earlier than MAT. Sandy tundra also had a sharp increase in NDVI in early growing season, only one period later during early June.

Several interesting patterns emerge upon summarizing NDVI indices along north–south gradients (Table 2). First, although the Atqasuk sandy sites show lower seasonal NDVI than the Barrow MAT site, they have earlier onset, and a longer growing season, which reflect the influence of temperature variation along the latitudinal gradient. Second, if the Atqasuk sandy site is placed with the SW Atqasuk MAT site, all indices fall between those of Barrow and Oumalik, which may reflect the actual zonal gradient along the western transect. Third, the MNT/MAT boundary at Oumalik and Sagwon can be clearly distinguished by peak NDVI, with approximately 20–30% difference between the two sites. A dramatic change of elevation occurs at this boundary. Finally, from Deadhorse to Franklin Bluffs,

Table 3
Summary of the regression analysis of biweekly series of NDVI anomalies vs. mean air temperature anomalies

Site	Type	NDVI vs. air T	r^2
Barrow	MNT	$y = 0.0152x + 0.0035$	0.39
	MAT	$y = 0.0196x + 0.0046$	0.52
Umiat	MAT	$y = 0.0031x + 0.0012$	0.09
Prudhoe	MNT	$y = 0.0078x + 0.0015$	0.40
W Kuparuk	MNT	$y = 0.0093x + 0.003$	0.30
Franklin Bluffs	MNT	$y = 0.0045x - 0.0028$	0.13
	MAT	$y = 0.0053x + 0.0021$	0.25
Sagwon Hill	MNT	$y = 0.0066x + 4e - 06$	0.18
	MAT	$y = 0.0063x + 0.0022$	0.17
Toolik Lake	MNT	$y = 0.0077x + 0.0007$	0.35
	MAT	$y = 0.0084x + 0.0033$	0.36

MAT = moist acidic tundra; MNT = moist nonacidic tundra.

NDVI greatly increases, which may reflect lower moss cover and strong cryoturbation around Deadhorse (Ping, Bockheim, Kimble, Michaelson, & Walker, 1998).

The relationship between NDVI and air temperature anomalies were found to be strongly positive, indicating the importance of growing season warmth to plant growth and biomass accumulation. Linear correlations were significant between biweekly NDVI and air temperature anomalies at Toolik Lake, Franklin Bluffs, and West Kuparuk. NDVI vs. air temperature yielded the highest regression coefficient. MNT had a higher correlation with warmth factors at Sagwon Hill than MAT, whereas MAT had the stronger correlations at Franklin Bluffs and Toolik Lake. MAT had higher NDVI overall along the temperature gradient than did MNT, as well as a higher intra-seasonal variability.

As shown in Table 3, greater variance was explained for most cases and in particular, Barrow and Sagwon Hill increased significantly. An $R^2 = 0.52$ was determined for the Barrow MAT site and $R^2 = 0.42$ for the Toolik MNT site. This indicates that intra-seasonal variability in NDVI is positively related to air temperatures, and the temperatures in early periods of the growing season have a greater contribution to NDVI variability.

4.7.4. Conclusions

NDVI values increase from late May, reach peaks around early August, and then decline from there. Onset starts earliest and higher peak NDVI occur at southern sites, and moist nonacidic tundra generally has lower NDVI values than moist acidic tundra throughout the growing seasons. Also, a major difference of NDVI occurs around the MNT–MAT boundary near Oumalik and Sagwon. Well-differentiated intra-seasonal NDVI curves make it a potential indicator for interpreting phenological features for different tundra types in Arctic Alaska.

A positive linear relationship was determined between biweekly NDVI and air temperature. MAT generally had a stronger correlation with seasonal temperatures compared to MNT.

Table 2
Summary of seasonal NDVI along latitudinal transects

Site	Peak NDVI		Onset date[a]		Green time (days)		Elevation (m)		N
	Mean	S.D.	Mean	S.D.	Mean	S.D.	Mean	S.D.	
MNT, western transect									
Barrow 1	0.396	0.020	170	1.68	88	2.49	6	0.66	9
SW Atqasuk 1	0.426	0.033	165	2.23	107	2.88	38	2.37	18
Oumalik 1	0.444	0.025	159	0.64	103	1.20	60	1.86	18
MAT/ST, western transect									
Barrow 2	0.437	0.012	170	0.94	88	2.47	11	0.85	9
Atqasuk 4	0.412	0.024	168	1.73	97	1.75	30	0.79	9
SW Atqasuk 2	0.495	0.012	159	0.70	109	1.99	48	3.52	18
Oumalik 2	0.546	0.010	159	0.70	105	1.87	100	3.74	27
Ivotuk 2	0.509	0.011	150	2.35	112	2.08	489	4.86	9
Ivotuk 3	0.563	0.006	152	1.43	110	1.73	609	5.05	9
MNT, eastern transect									
Deadhorse 1	0.321	0.021	170	1.26	87	2.16	15	0.79	9
FB 1	0.445	0.011	169	1.22	90	1.51	94	4.34	27
Sagwon 1	0.457	0.013	159	1.33	101	1.91	182	3.12	27
Toolik 1	0.449	0.009	148	0.97	114	1.75	651	5.48	9
MAT/ST, eastern transect									
FB 2	0.488	0.005	165	1.57	97	1.39	224	5.08	18
Sagwon 2	0.527	0.006	155	1.96	105	2.26	313	7.08	27
Toolik 2	0.511	0.009	148	1.12	116	0.91	588	2.76	9
Toolik 3	0.564	0.012	156	1.94	106	1.62	772	6.49	9
MNT–MAT boundary									
Oumalik 1	0.444	0.025	159	0.64	103	1.20	60	1.86	18
Oumalik 2	0.546	0.010	159	0.70	105	1.87	100	3.74	27
Sagwon 1	0.457	0.013	159	1.33	101	1.91	182	3.12	27
Sagwon 2	0.527	0.006	155	1.96	105	2.26	313	7.08	27

1: MNT, 2: MAT, 3: shrub tundra, 4: sandy tundra; FB: Franklin Bluffs.
[a] In Julian date.

4.8. Satellite-derived greenness rate of change across the North Slope of Alaska in the 1990s (D. Stow, A. Hope, S. Daeschner, A. Petersen, and D. Douglas)

4.8.1. Introduction

Site-specific analyses of Arctic tundra ecosystems of the North Slope have yielded evidence of increases in the cover and stature of low stature shrubs, possibly as a response to climatic warming over the past three decades (Sturm et al., 2001). While characteristically low in stature, shrubs are the tallest plant form within Arctic tundra ecosystems of the North Slope and have been shown to have the greatest influence on NDVI (Hope et al., 1993). Thus, if shrub cover and/or stature have increased throughout areas of the North Slope over the past few decades, time series of satellite-derived NDVI may reveal increased greenness for such areas.

The objective of this case study is to demonstrate the utility of a NDVI time series derived from AVHRR LAC imagery captured between 1990 and 1999, for determining areas of rapidly changing greenness that may be due to increases in shrub cover and/or stature. Greenness trends across the North Slope were examined at a finer (1 km) spatial resolution than has been achieved with previous studies based on AVHRR global area coverage (GAC) data sets 4 to 8 km spatial resolution (see Section 4.9). The AVHRR LAC data set analyzed in the case study is an improved version of that generated by the USGS EROS Data Center (EDC), which have been utilized in similar studies (see Section 4.7).

4.8.2. Data and methods

An NDVI time series was produced for the North Slope region for growing seasons in the 1990s by assembling AVHRR LAC images from several sources. This was accomplished by: (1) refining AVHRR maximum value composite NDVI products (Holben, 1986) generated by the USGS EDC for the period July 1990 through October 1995 and April through October 1997, and (2) augmenting these data sets by producing MVCs for April through June 1990 and the growing seasons of 1996, 1998, and 1999. Only data from afternoon (NOAA-11 and -14) and near-nadir overpasses were incorporated in the composites. Calibration coefficients for NOAA-11 were based on Vermote and Kaufman (1995) and on Mitchell (1999) for NOAA-14. A twice monthly (15 or 16 days) compositing interval was used for 1990 through 1994 and a 14-day interval for 1995–1999.

Stratospheric aerosol effects on NDVI for 1991–1993 caused by the eruption of Mt. Pinatubo (Hope et al., 2003) were reduced by cross-calibrating with AVHRR NDVI GAC data developed by the Global Inventory Monitoring and Modeling Systems (GIMMS) group at NASA Goddard Space Flight Center (GSFC) (Vermote & El Saleous, 1994). The GIMMS correction procedure was based on the assumptions that optical depth of stratospheric aerosols is longitudinally constant and that

bright cloud and dark ocean pixels are suitable as calibration points.

AVHRR LAC (1 km) pixels were spatially aggregated by averaging 3×3 blocks of pixels to minimize misregistration effects. The 3 km NDVI MVC raster data were integrated (i.e., per-pixel summation) over each growing season to derive maps of seasonally integrated normalized difference vegetation index (SINDVI) for each growing season of the 1990s. The integration period was defined as the series of MVC pixels for which NDVI exceeded the value of 0.1 within the potential growing season from April through October. A number of studies confirm that integration or summation of the NDVI over a growing season is correlated with above ground, net primary production (Goward & Dye, 1987) and primary productivity of different Arctic tundra communities is highly variable (Webber, 1977).

The greenness rate of change (GRC), defined as the slope of the least squares line fitting the interannual variability of SINDVI values over the 10-year time period, was calculated for each 3 km pixel by the least squares method. A t-value was also calculated for each pixel to determine if the GRC slope was statistically significant from zero.

4.8.3. Results

A gradually increasing and statistically significant SINDVI trend (i.e., moderately increasing GRC) of +0.8 per year, or 3% increase per year from the 1990 baseline for the North Slope was observed (Stow et al., 2003). The foothills province of the North Slope exhibited a significant GRC trend of +0.10 per year and the trend for the coastal plain province is not significantly different from zero.

Fig. 15 is a map showing areas of highest GRC values for the entire North Slope as red pixels overlaid on a general vegetation map. Red pixels are those that meet two criteria: (1) top 5% frequency of occurrence of GRC values (which all had significant trend slopes) and (2) have at least two adjacent pixels that also meet criterion 1.

Over 95% of these pixels representing the most rapid increases in net primary production are located in the foothills province and 85% within the vegetation class moist tussock and dwarf shrub tundra, as mapped by Fleming (2000). Only 5% of these rapidly greening pixels are associated with the shrub dominant, dwarf shrub tundra class. A hypothesis for explaining this results is that shrub cover and stature have increased most rapidly within areas where graminoid vegetation (e.g., classic tussock tundra) have been dominant but heavily interspersed with dwarf shrubs. Interestingly, the greatest concentration of the pixels with the highest GRC values are located within the foothills of the Kuparuk River watershed, the most heavily studied portion of the North Slope region (Reynolds & Tenhunen, 1996).

4.8.4. Conclusions

An increasing SINDVI trend over the 1990s may be accentuated by several factors including: (1) depressed NDVI levels following the eruption of Mt. Pinatubo, (2) changes in
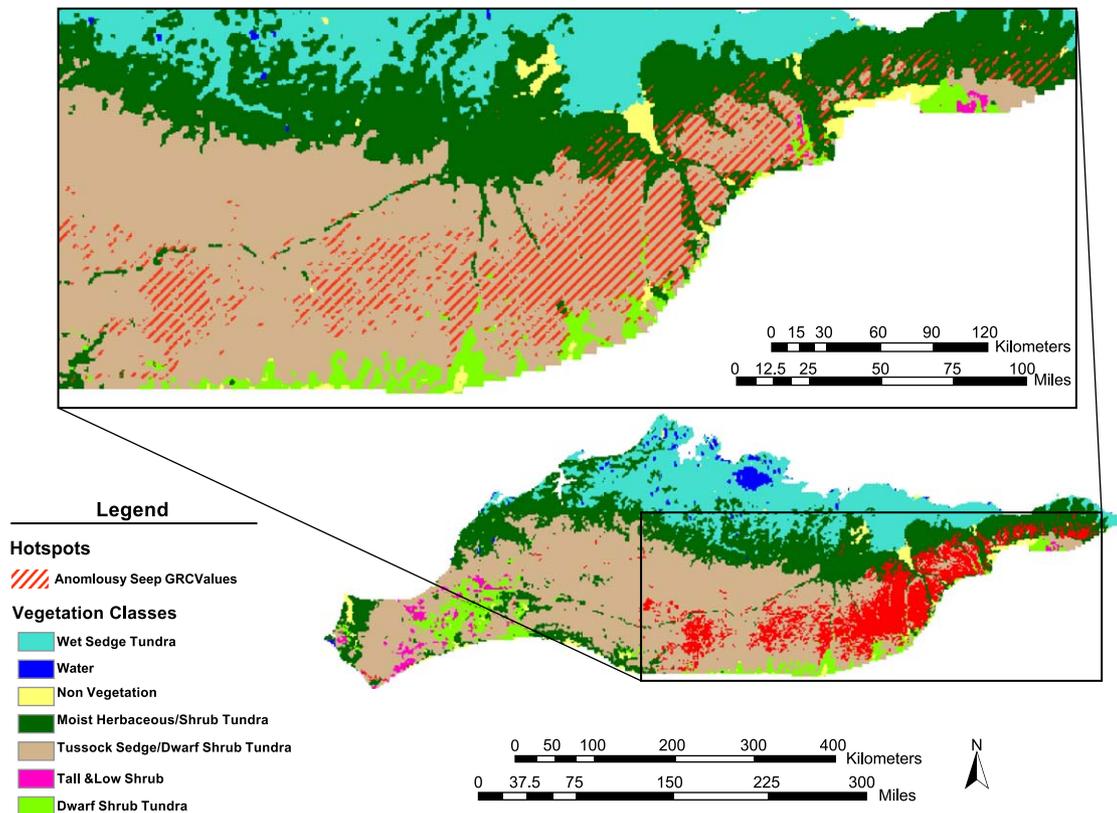
Fig. 15. Map portraying greenness rate of change (GRC) of seasonally integrated normalized difference vegetation index (SINDVI) for the North Slope region. The top 5% of pixels with steepest GRC are shown in red, overlain on a general tundra vegetation and land cover type map produced by Fleming (2000). An area of the eastern North Slope region exhibiting the greatest amount of rapidly greening pixels is shown enlarged on top.

the radiometric calibration relationship for NOAA-14 AVHRR over time, and (3) drift and differences in the time of acquisition and therefore, solar zenith angle (SZA), for NOAA-11 and NOAA-14 satellites (Stow et al., in press). An attempt was made to minimize these effects on SINDVI values and the results of other studies utilizing standard USGS NDVI MVC data sets may be suspect (Cihlar et al., 1998). After implementing corrections for the stratospheric aerosol effect from the Mt. Pinatubo eruption and adjusting for changes in radiometric calibration coefficients, an apparent increasing trend of SINDVI in the 1990s is evident for the entire North Slope. The most pronounced increase is observed for the foothills physiographic province, particularly in the eastern half of this province. Approaches based on higher spatial resolution sensing (such as were summarized in previous case studies in this paper) should be implemented to test the hypothesis that these areas of highest GRC are undergoing an increase in the cover and/or stature of shrubs.

4.9. Satellite-inferred increased activity of arctic tundra between 1982 and 1999 (Liming Zhou and Ranga B. Myneni)

4.9.1. Introduction

Due to the cold, desert-like conditions and short growing seasons, Arctic tundra ecosystems are extremely sensitive to disturbances. Pronounced high-latitude warming and associated reduction in snow cover and earlier melting of snow (Groisman et al., 1994; Hansen et al., 1999) during the past two decades may have affected the photosynthetic activity of Arctic tundra.

Myneni et al. (1997) and Zhou, Tucker et al. (2001), Zhou, Kaufmann, Tian, Myneni, and Tucker (2003) report that the photosynthetic activity of terrestrial vegetation between 40°N and 70°N increased in 1980s and 1990s and this increase was linked to changes in land surface temperature. However, forests are the major contributors to such increase and whether Arctic tundra has experienced similar changes is unknown. For this case study, AVHRR data are used to infer interannual variations of Arctic tundra photosynthetic activity beyond 70°N from 1982 to 1999.

4.9.2. Data and methods

A continental NDVI data set at 8 km resolution for the years 1982 to 1999 produced by the Global Inventory Monitoring and Modeling Studies (GIMMS) group from AVHRR onboard the afternoon-viewing NOAA series satellites (NOAA 7, 9, 11, and 14) was used (Tucker et al., 2001; Zhou et al., 2001). The data processing included improved navigation, sensor calibration, and atmospheric corrections. A technique based on data from high cold clouds and dark ocean was used to calibrate the data set
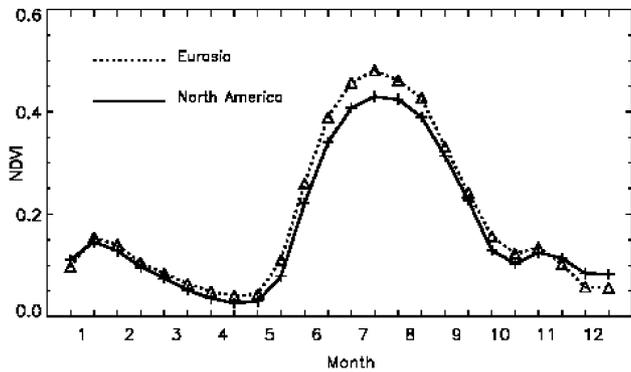
Fig. 16. Spatial averaged NDVI annual cycle over tundra pixels beyond 60°N between 1982 and 1999 in North America and Eurasia.

(Vermote & Kaufman, 1995). This calibration was improved by a method developed by Los (1998). The data for the periods April 1982–December 1984 and June 1991–December 1993 were corrected to remove the effects of stratospheric aerosol loading from El Chicon and Mt. Pinatubo eruptions (Vermote & El Saleous, 1994). The maximum NDVI value during a 15-day composite period was extracted for each 8 km pixel. These data generally correspond to observations in the forward, nearest to near-nadir view directions (Los, Justice, & Tucker, 1994) and clear atmospheres (Holben, 1986). This method helps minimize surface bidirectional reflectance effects and residual atmospheric effects. Further technical discussion on the quality of this data set can be found in Tucker et al. (2001) and Zhou et al. (2001).

A global land-surface temperature data during the same period at 2°×2° resolution was also used to support the results from the NDVI data analysis. This data set was produced by the NASA Goddard Institute for Space Studies (GISS) and is in the form of monthly anomalies with respect to the 1951–1980 mean (Hansen et al., 1999).

4.9.3. Results

First, all pixels at 8 km resolution beyond 60°N were labeled into "tundra" and "non-tundra" classes according to a land cover map at 1°×1° spatial resolution (DeFries & Townshend, 1994). Due to the coarse resolution of the land cover map, "tundra" pixels were defined as those with (1) June to September composite NDVI values >0.1 in each year and (2) June to September average NDVI values >0.2 for all years to reduce nonvegetation effects on NDVI from snow and barren lands. These criteria are based on analyses of the growing season NDVI values over deserts and semi-deserts (Zhou et al., 2001). This method also reduces the sensitivity of NDVI to changes in solar zenith angle (Kaufmann et al., 2000) and artifacts due to temporal variations in ground reflectivity in sparsely vegetated areas. As a result, there are 22,743 tundra pixels (1.5×10^6 km^2) in Eurasia and 7817 tundra pixels (5×10^5 km^2) in North America.

Second, the growing season was defined according to the 18-year average NDVI annual cycle over all Arctic tundra pixels beyond 60°N. Fig. 16 shows that NDVI increases steadily from May, reaches its peak at the end of July and the beginning of August, and then declines. There is a spurious NDVI decrease from January to April due to high solar zenith angle and snow cover. Therefore, the growing season was defined as June to September (snow-free period). Any Arctic tundra pixel with a NDVI less than 0.2 during the growing season will be excluded to minimize snow effects upon spatial and temporal averaging.

Next, NDVI data for the Artic tundra pixels were spatially aggregated to quarter degree grids and temporally averaged over the growing season. Fig. 17 shows the spatial pattern of growing season NDVI trends at 0.25° resolution. In general, NDVI of most pixels shows an increasing trend. Pixels with the largest NDVI increase (in red and purple) during the sample period are noteworthy in north Russia, especially along a broad swath of land between 70°E and 140°E and north of 65°N, the Alaska North Slope, and parts of northern Canada and Scandinavia. NDVI decreases are observed over some areas in eastern Siberia, northwestern Russia, and northwestern Canada.

Annual series of growing season NDVI beyond 60°N were generated by spatially averaging all tundra pixels with composite NDVI values >0.2. The upward trend is shown in both Eurasia and North America (Fig. 18). Linear time trends in NDVI estimated by ordinary least squares from
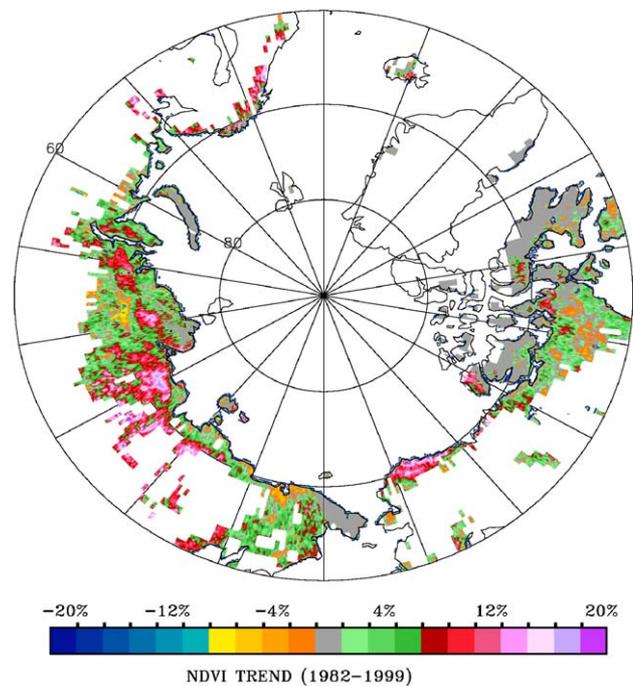

Fig. 17. Spatial patterns of NDVI trend from 1982 to 1999 during the growing season defined as June to September over tundra pixels beyond 60°N.
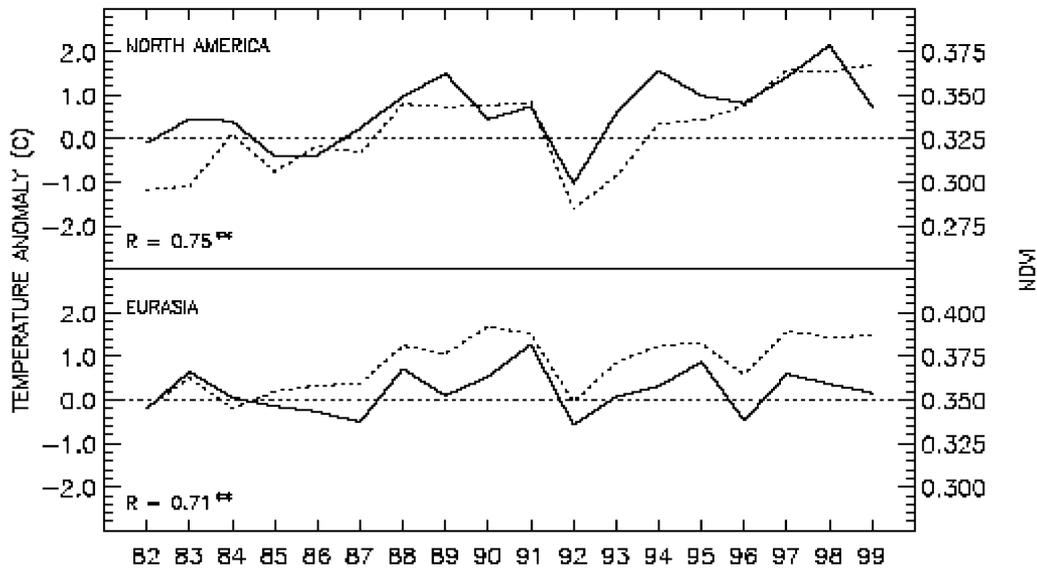
Fig. 18. Spatially averaged NDVI (dotted line) and near-surface air temperature anomaly (solid line) for arctic tundra beyond 60°N during June to September. R is the correlation coefficient. The double asterisk (single asterisk) denotes the statistical significance at the 1% (5%) level.

1982 to 1999 show that NDVI in Eurasia and North America increased by 10% and 17%, respectively, with a statistical significance at the 5% level. North American NDVI has a larger increase than Eurasian NDVI but with a larger deviation.

Finally, annual series of growing season temperature beyond 60°N are generated similarly to those of NDVI (Fig. 18). On both continents, the growing season NDVI is positively correlated with the temperature anomaly, with correlation coefficients of 0.75 in North America and 0.71 in Eurasia at the 1% significance level. Changes in NDVI likely reflect changes in biological activity because NDVI are consistent with ground-based measurements of temperature, an important determinant of biological activity.

The annual integral of NDVI is a proxy for vegetation photosynthetic activity over the entire growing season (Fung, Tucker, & Prentice, 2001). An increase in averaged growing season NDVI can be characterized as the annual integral of NDVI during the growing season, and thus an increase in growing season average NDVI may indicate a photosynthetic gain.

4.9.4. Conclusions

During the past 18 years, satellite NDVI data in Arctic regions suggest an increase in photosynthetic activity by Arctic tundra ecosystems over most areas beyond 60°N and some of this increase could be attributed to the warming in this region. This inference may be valid at the continental scale but the effects of other factors such as precipitation and drought may be also accounted for the observed NDVI changes at the regional scale. In addition, some nonvegetation signals, especially variations in solar-viewing geometry and effects of clouds and snow, may still remain in the satellite NDVI data. Additional corroboration from in situ data and further study are required.

5. Conclusions

By presenting theoretical and technical background sections and nine case studies, this paper provides a synthesis of the goals, issues, and key findings associated with some examples of multi-temporal analyses of Arctic tundra ecosystems using data from optical remote sensing systems at a myriad of spatial and temporal scales. Though the techniques for capturing, processing, and analyzing remotely sensed data are not unique to, or developed specifically for, sensing of Arctic lands, some of the environmental factors that tend to make remote sensing challenging are unique or particularly relevant. Data from optical remote sensing systems operating in the visible, near infrared, and short-wave infrared portions of the spectrum provide the greatest information content about ecosystem change, particularly with regards to aspects of vegetation composition, condition, and composition. However, optical sensing of land surfaces from satellite and most aircraft platforms is challenging due to prevalent cloud cover precluding data collection.

Case studies within this paper demonstrate that ground-level sensors on stationary or moving track platforms and wide-swath imaging sensors on polar orbiting satellites are particularly useful for capturing optical remote sensing data at sufficient frequency to study tundra vegetation dynamics and changes for the cloud prone Arctic. Less frequent imaging with high spatial resolution instruments on aircraft and lower orbiting satellites enable more detailed analyses of land cover change and calibration/validation of coarser resolution observations.

The strongest signals of ecosystem change detected thus far appear to correspond to an apparent expansion of tundra shrubs and changes in the amount and extent of thaw lakes and ponds. Changes in shrub cover and extent

have been documented by modern repeat imaging that matches archived historical aerial photography. Such historical imagery provides a baseline record starting from up to 70 years B.P. and where available, will provide the longest potential record length for determining shifts in tree-line at the Arctic–Subarctic interface. NOAA AVHRR time series provide a 20-year record for determining changes in greenness that relates to photosynthetic activity, net primary production, and growing season length. However, the use of satellite data and SVIs to estimate regional-scale patterns of biophysical quantities requires field measurements to establish the basic predictive model. These models are likely to be scale and sensor dependent and their use with data from satellites may incur substantial uncertainty. Furthermore, obtaining samples large enough to represent the spatial heterogeneity of natural ecosystems is challenging given the logistical difficulties of collecting field data in Arctic ecosystems. The strong contrast between land materials and surface waters enables changes in lake and pond extent to be readily measured and mapped. Though outside the scope of this paper, synthetic aperture radar systems that enable high spatial resolution imaging through clouds are particular promising for future assessment of surface water changes.

Remotely sensed data from newer or future generation optical sensors should increase the ability of Arctic scientists to derive spatially-explicit information on changes of tundra ecosystems. In particular, the Moderate Resolution Imaging Spectrometer (MODIS) on the TERRA and AQUA satellites are beginning to provide a readily available time series of image derived products for examining regional-scale changes in properties and composition of Arctic tundra ecosystems. The fairly recent availability of satellite data with very high spatial resolution (1 to 5 m), such as IKONOS and QuickBird multispectral data, is likely to further enhance more detailed analyses of Arctic land cover changes.

References

Arft, A. M., Walker, M. D., Gurevitch, J., Alatalo, J. M., Bret-Harte, M. S., Dale, M., Diemer, M., Gugerli, F., Henry, G. H. R., Jones, M. H., Hollister, R. D., Jonsdottir, I. S., Laine, K., Levesque, E., Marion, G. M., Molau, U., Molgaard, P., Nordenhall, U., Razzhivin, V., Robinson, C. H., Starr, G., Stenstrom, A., Stenstrom, M., Totland, O., Turner, L., Walker, D., Webber, P. J., Welker, J., & Wookey, P. A. (1999). Response patterns of tundra plant species to experimental warming: A meta-analysis of the International Tundra Experiment. *Ecological Monographs*, *69*, 491–511.

Baglio, J. V., & Holroyd III, E. W. (1989). Methods for operational snow cover area mapping using the advanced very high resolution radiometer: San Juan mountains test study. *Research Technical Report, U.S. Geological Survey*. Sioux Falls: EROS Data Center.

Bliss, L. C., & Matveyeva, N. V. (1992). Circumpolar arctic vegetation in Arctic. In F. S. Chapin (Ed.), *Arctic ecosystems in a changing climate: An ecolophysiological perspective* (pp. 59–89). San Diego: Academic Press.

Bret-Harte, M. S., Shaver, G. R., Zoerner, J. P., Johnstone, J. F., Wagner, J. L., Chavez, S., Gunkelman, R. F., Lippert, S. C., & Laundre, J. A. (2001). Developmental plasticity allows *Betula nana* to dominate tundra subjected to an altered environment. *Ecology*, *82*, 18–32.

Brown, J., Everett, K. R., Webber, P. J., Maclean Jr., S. F., & Murray, D. F. (1980). The coastal tundra at Barrow. In J. Brown, P. C. Miller, L. L. Tieszen, & L. F. Bunnell (Eds.), *An arctic ecosystem: The coastal Tundra at Barrow, Alaska* (pp. 1–29). Stroudsburg, PA: Dowden, Hutchinson & Ross.

Cameron, R. D., & Whitten, K. R. (1980). Nutrient dynamics of caribou forage on Alaska's Arctic Slope. In E. Reimers, E. Gaare, S. Skjenneberg*Proceedings of the Second International Reindeer/Caribou Symposium, September 1979, Roros (Norway)* (pp. 159–166). Trondheim: Direktoratet for vilt og ferskvannsfisk.

Chan-McLeod, A. C. A., White, R. G., & Holleman, D. F. (1994). Effects of protein and energy intake, body condition, and season on nutrient partitioning and milk production in caribou and reindeer. *Canadian Journal of Zoology*, *72*, 938–947.

Chan-McLeod, A. C. A., White, R. G., & Russell, D. E. (1999). Comparative body composition strategies of breeding and non-breeding female caribou. *Canadian Journal of Zoology*, *77*, 1901–1907.

Chapin III, F. S., & Shaver, G. R. (1996). Physiological and growth responses of Arctic plants to a field experiment simulating climatic change. *Ecology*, *77*, 822–840.

Chapin III, F. S., Shaver, G. R., Giblin, A. E., Nadelhoffer, K. J., & Laundre, J. A. (1995). Responses of Arctic tundra to experimental and observed changes in climate. *Ecology*, *73*(3), 694–711.

Chapman, W. L., & Walsh, J. E. (1993). Recent variations of sea ice and air temperatures in high latitudes. *Bulletin of the American Meteorological Society*, *74*, 33–47.

Cihlar, J., Chen, J. M., Li, Z., Huang, F., Latifovic, R., & Dixon, R. (1998). Can interannual land surface signal be discerned in composite AVHRR data? *Journal of Geophysical Research*, *103*(D18), 23163–23172.

DeFries, R. S., & Townshend, J. R. G. (1994). NDVI-derived land cover classification at a global scale. *International Journal of Remote Sensing*, *15*, 3567–3586.

Donoghue, D. N. M. (2000). Remote sensing: Sensors and applications. *Progress in Physical Geography*, *24*(3), 407–414.

Eidenshink, J. C., & Faundeen, J. L. (1994). The 1 km AVHRR global land data set: First stages of implementation. *International Journal of Remote Sensing*, *15*(17), 3443–3462.

Fancy, S. G., Pank, L. F., Whitten, K. R., & Regelin, W. L. (1989). Seasonal movements of caribou in arctic Alaska as determined by satellite. *Canadian Journal of Zoology*, *67*, 644–650.

Fleming, M. (2000). Metadata for Statewide Vegetation Map of Alaska, USGS EROS Data Center, Anchorage, Alaska ⟨http://www.agdc.usgs.gov/data/projects/fhm//vegcls.txt⟩.

Forbes, B. C., Ebersole, J. J., & Standberg, B. (2001). Anthropogenic disturbance and patch dynamics in circumpolar Arctic ecosystems. *Conservation Biology*, *15*(4), 954–969.

Fung, I. Y., Tucker, C. J., & Prentice, K. C. (2001). Application of very high resolution radiometer vegetation index to study atmosphere-biosphere exchange of CO_2. *Journal of Geophysical Research*, *92*, 2999–3015.

Goel, N. S. (1985). Inversion of canopy reflectance models for estimation of biophysical parameters from reflectance data. In G. Asrar (Ed.), *Theory and applications of optical remote sensing* (pp. 205–251). New York: Wiley, Ch. 6.

Goward, S., & Dye, D. (1987). Evaluating North America net primary productivity with satellite observations. *Advances in Space Research*, *7*, 165–174.

Gower, S. T., Kucharik, C. J., & Norman, J. M. (1999). Direct and indirect estimation of leaf area index f(APAR), and net primary production of terrestrial ecosystems. *Remote Sensing of Environment*, *70*(1), 29–51.

Griffith, B., Douglas, D. C., Walsh, N. E., Young, D. D., McCabe, T. R., Russell, D. E., White, R. G., Cameron, R. D., & Whitten, K. D. (2002). The Porcupine caribou herd. In: D. C. Douglas, P. E. Reynolds, & R. B. Rhode (Eds.), *Refuge coastal plain terrestrial wildlife research summa-*

ries. U.S. geological survey, biological science report USGS/BRD/BSR-2002-0001 (pp. 8–37). Anchorage: US Geological Survey.

Groisman, P. A., Karl, T. R., & Knight, R. W. (1994). Observed impact of snow cover on the heat balance and rise of continental spring temperatures. *Science, 263*, 198–200.

Hall, F. G., Strebel, D. E., Nickeson, J. E., & Goetz, S. J. (1991). Radiometric rectification: Toward a common radiometric response among multi-date, multi-sensor images. *Remote Sensing of Environment, 35*, 11–27.

Hansen, J., Ruedy, R., Glascoe, J., & Sato, M. (1999). GISS analysis of surface temperature change. *Journal of Geophysical Research, 104*, 30997–31022.

Hinzman, L. (2001). ⟨www http://arcss.colorado.edu⟩.

Hinzman, L. D., Yoshikawa, K., & Kane, D. L. (2001). Hydrologic response and feedbacks to a warmer climate in arctic regions. Proceedings of the second Wadati conference on global change and polar climate, 7–9 March 2001, Tsukuba (Japan).

Hobbie, S. E., & Chapin III, F. S. (1998). The response of tundra plant biomass, aboveground production, nitrogen, and CO_2 flux to experimental warming. *Ecology, 79*, 1526–1544.

Holben, B. N. (1986). Characteristics of maximum-value composite images from temporal AVHRR data. *International Journal of Remote Sensing, 7*, 1417–1434.

Hope, A., Boynton, W., Stow, D., & Douglas, D. (2003). Interannual growth dynamics of vegetation in the Kuparuk River watershed based on the normalized difference vegetation index. *International Journal of Remote Sensing, 24*(17), 3413–3425.

Hope, A., Coulter, L., & Stow, D. (1999). Estimating lake area in an arctic landscape using linear mixture modelling with AVHRR data. *International Journal of Remote Sensing, 20*, 829–835.

Hope, A., & Stow, D. (1995). Shortwave reflectance properties of Arctic tundra. In J. Reynolds, & J. Tenhuenen (Eds.), *Landscape function and disturbance in Arctic tundra. Ecological Studies*, vol. 120, (pp. 155–164). Heidelberg: Springer.

Hope, A. S., Kimball, J. S., & Stow, D. A. (1993). Relationship between tussock tundra spectral reflectance properties and biomass and vegetation composition. *International Journal of Remote Sensing, 14*, 1861–1874.

Hope, A. S., Pence, K. R., & Stow, D. A. (in press). NDVI from low altitude aircraft and composited NOAA AVHRR data for scaling Arctic ecosystem fluxes. *International Journal of Remote Sensing*.

Houghton, J. T., Meira Fihlo, L. G., Callender, B. A., Harri, N., Kattenberg, A., & Maskell, K. (1996). *Climate change 1995: The science of climate change*. Cambridge: University Press.

Jeyaseelan, A. T., & Thiruvengadachari, S. (1993). Suspected Mt. Pinatubo aerosol impact on NOAA AVHRR NDVI over India. *International Journal of Remote Sensing, 14*(3), 603–608.

Jia, G. J., Epstein, H. E., & Walker, D. A. (2002). Spatial characteristics of AVHRR-NDVI along latitudinal transects in Northern Alaska. *Journal of Vegetation Science, 13*, 315–326.

Jia, G. J., Epstein, H. E., & Walker, D. A. (in press). Controls over intra-seasonal dynamics of AVHRR-NDVI for the Arctic Tundra in Northern Alaska. *International Journal of Remote Sensing*.

Johnson, R. D., & Kasischke, E. S. (1998). Change vector analysis: A technique for the multispectral monitoring of land cover and condition. *International Journal of Remote Sensing, 19*, 411–426.

Kattenburg, A., Giorgi, F., Grassl, H., Meehl, G. A., Mitchell, J. F. B., Stouffer, R. J., Tokioka, T., Weaver, A. J., & Wigley, T. M. L. (1996). Climate models—projections of future climate. In J. T. Houghton, L. G. Meira Filho, B. A. Callander, N. Harris, A. Kattenburg, & K. Maskell (Eds.), *Climate change 1995 the science of climate change. The second assessment report of the IPCC: Contribution to working group 1* (pp. 285–357). Cambridge: University Press.

Kaufmann, R. K., Zhou, L., Knyazikhin, Y., Shabanov, N. V., Myneni, R. B., & Tucker, C. J. (2000). Effect of orbital drift and sensor changes on the time series of AVHRR vegetation index data. *IEEE Transactions on Geoscience and Remote Sensing, 38*(6), 2584–2597.

Keeling, C. D., Chin, J. F. S., & Whorf, T. P. (1996). Increased activity of northern vegetation inferred from atmospheric CO_2 measurements. *Nature, 382*, 146–149.

Lachenbruch, A. H., & Marshell, B. V. (1986). Changing climate: Geothermal evidence from permafrost in the Alaskan Arctic. *Science, 234*, 689–696.

Land–Atmosphere–Ice Interactions (LAII) (2001). Changes in the Arctic Land–Atmosphere System: The Role of Physical, Biological, and Biogeochemical Couplings in the Arctic. Draft Science Plan ⟨www http://www.laii.uaf.edu/pubs/smo-pubs/draftplan.pdf⟩.

Law, B. E., & Waring, R. H. (1994). Combining remote-sensing and climatic data to estimate net primary production across Oregon. *Ecological Applications, 4*(4), 717–728.

Lloyd, A. H., & Fastie, C. L. (2002). Spatial and temporal variability in the growth and climate response of treeline trees in Alaska. *Climatic Change, 52*, 481–509.

Lloyd, A. H., Rupp, T. S., Fastie, C. L., & Starfield, A. M. (in press). Patterns and dynamics of treeline advance in the Seward Peninsula, Alaska. *Journal of Geophysical Research*.

Loeb, N. G. (1997). In-flight calibration of NOAA AVHRR visible and near-IR bands over Greenland and Antarctica. *International Journal of Remote Sensing, 18*, 477–490.

Los, S. O. (1998). Estimation of the ratio of sensor degradation between NOAA AVHRR channel 1 and 2 from monthly NDVI composites. *IEEE Transactions on Geoscience and Remote Sensing, 36*, 202–213.

Los, S. O., Justice, C. O., & Tucker, C. J. (1994). A global $1° \times 1°$ NDVI data set for climate studies derived from the GIMMS continental NDVI data. *International Journal of Remote Sensing, 15*, 3493–3518.

Malila, W. A. (1980). Change vector analysis: An approach for detecting forest changes with Landsat. Proceedings, LARS machine processing of remotely sensed data symposium, W. Lafayette, Indiana, US. (pp. 326–336).

Markon, C. J., Fleming, M. J., & Binnian, E. F. (1995). Characteristics of vegetation phenology over the Alaskan landscape using AVHRR time-series data. *Polar Record, 31*(177), 179–190.

Maxwell, B. (1992). Arctic climate: Potential for change under global warming. In J. F. Reynolds, G. R. Shaver, & J. Svoboda (Eds.), *Arctic ecosystems in a changing climate* (pp. 11–34). San Diego: Academic Press.

McGuffie, K., & Henderson-Sellers, A. (1986). Illustration of the influence of shadowing on high latitude information derived from satellite imagery. *International Journal of Remote Sensing, 7*, 1359–1365.

McMichael, C., Hope, A., Stow, D., Fleming, J., Vourlitis, G., & Oechel, W. (1999). Estimating CO_2 exchange in Arctic Tundra ecosystems using a spectral vegetation index. *International Journal of Remote Sensing, 20*, 683–698.

Mitchell, R. M. (1999). CSIRO Atm. Res ⟨http://www.dar.csiro.au/rs/CalWatch/calwatch.html⟩.

Moffitt, F. H. (1970). *Photogrammetry* (2nd ed.). Scranton, PA: International Textbook.

Muller, S. V., Racoviteanu, A. E., & Walker, D. A. (1999). Landsat MSS-derived land-cover map of northern Alaska: Extrapolation methods and a comparison with photo-interpreted and AVHRR-derived maps. *International Journal of Remote Sensing, 20*, 2921–2946.

Myneni, R. B., & Asrar, G. (1994). Atmospheric effects and spectral vegetation indices. *Remote Sensing of Environment, 47*, 390–402.

Myneni, R. B., Keeling, C. D., Tucker, C. J., Asrar, A., & Nemani, R. R. (1997). Increased plant growth in the northern high latitudes from 1981 to 1991. *Nature, 386*, 698–702.

Nemani, R. R., Pierce, L., Band, L. E., & Running, S. W. (1993). Forest ecosystem processes at the watershed scale: Sensitivity to remotely sensed leaf area index observations. *International Journal of Remote Sensing, 14*, 2519–2534.

Nemani, R. R., & Running, S. W. (1997). Landcover characterization using multi-temporal red, near-IR and thermal-IR data from NOAA/AVHRR. *Ecological Applications, 7*(1), 79–90.

Noyle, B. M. (1999). *The Vegetation and a Landsat Assisted Vegetation Map of the Barrow Peninsula, Northern Alaska*. Michigan State University: Master of Science Thesis, 183 pp.

Oechel, W. C., Vourlitis, G. L., Hastings, S. J., & Bochkarey, S. A. (1995). Change in Arctic CO_2 flux over two decades: Effects of climate change at Barrow, Alaska. *Ecological Applications*, 5, 846–855.

Parker, K. L., White, R. G., Gillingham, M. P., & Holleman, D. F. (1990). Comparison of energy metabolism in relation to daily activity and milk consumption by caribou and muskox neonates. *Canadian Journal of Zoology*, 68, 106–114.

Ping, C. L., Bockheim, J. G., Kimble, J. M., Michaelson, G. J., & Walker, D. A. (1998). Characteristics of cryogenic soils along a latitudinal transect in Arctic Alaska. *Journal of Geophysical Research*, 103, 28917–28928.

Privette, J. L., Fowler, C., Wick, G. A., Baldwin, D., & Emery, W. J. (1995). Effects of orbital drift on advanced very high resolution radiometer products: Normalized difference vegetation index and sea surface temperature. *Remote Sensing of Environment*, 53, 164–171.

Randerson, J. T., Field, C. B., Fung, I. Y., & Tans, P. P. (1999). Increases in early season ecosystem uptake explain recent changes in the seasonal cycle of atmospheric CO_2 at high northern latitudes. *Geophysical Research Letters*, 26, 2765–2768.

Reynolds, J. F., & Tenhunen, J. D. (1996). Ecosystem response, resistance, resilience, and recovery in Arctic landscapes: Introduction. In J. F. Reynolds, & J. Tenhunen (Eds.), *Landscape function and disturbance in Arctic Tundra. Ecological Studies*, vol. 120 (pp. 3–18). Heidelberg: Springer.

Roa, C., & Chen, J. (1999). Revised post-launch calibration of the visible and near-infrared channels of the Advanced Very High Resolution Radiometer on the NOAA-14 spacecraft. *International Journal of Remote Sensing*, 20, 3485–3491.

Sellers, P. J. (1985). Vegetation-canopy spectral reflectance and biophysical processes. In G. Asrar (Ed.), *Theory and applications of optical remote sensing* (pp. 297–335). New York: Wiley, Ch. 8.

Serreze, M. C., Walsh, J. E., Chapin III, F. S., Osterkamp, T., Dyurgerov, M., Romanovsky, V., Oechel, W. C., Morison, J., Zhang, T., & Barry, R. G. (2000). Observational evidence of recent change in the northern high-latitude environment. *Climatic Change*, 46, 159–207.

Shabanov, N., Zhou, L., Knyazikhin, Y., Myneni, R., & Tucker, C. (2002). Analysis of interannual changes in northern vegetation activity observed in AVHRR data during 1981 to 1994. *IEEE Transactions on Geoscience and Remote Sensing*, 40, 115–130.

Shibayama, M., Salli, A., Hame, T., Iso-Livari, L., Morinaga, S., Inoue, Y., & Akiyama, T. (1995). Spectral detection of subarctic vegetation phenophases. *IEEE Transactions on Geoscience and Remote Sensing*, 1488–1490.

Shippert, M. M., Walker, D. A., Auerbach, N. A., & Lewis, B. E. (1995). Biomass and leaf-area index maps derived from SPOT images for Toolik Lake and Imnavait Creek areas, Alaska. *Polar Record*, 31, 147–154.

Silapaswan, C. S., Verbyla, D. L., & McGuire, A. D. (2001). Land cover change on the Seward Peninsula: The use of remote sensing to evaluate the potential influences of climate warming on historical vegetation dynamics. *Canadian Journal of Remote Sensing*, 27, 542–554.

Spanner, M. A., Pierce, L. L., Peterson, D. L., & Running, S. W. (1990). Remote sensing of temperate coniferous forest leaf area index: The influence of canopy closure, understory vegetation, and background reflectance. *International Journal of Remote Sensing*, 11, 95–111.

Stone, R. S., Dutton, E. G., Harris, J. M., & Longenecker, D. (2002). Earlier spring snowmelt in northern Alaska as an indicator of climate change. *Journal of Geophysical Research*, 107(D10).

Stow, D., Daeschner, S., Hope, A., Douglas, D., Petersen, A., Myneni, R., Zhou, L., & Oechel, W. (2003). Variability of the seasonally integrated normalized difference vegetation index across the North Slope of Alaska in the 1990s. *International Journal of Remote Sensing*, 24(5), 1111–1117.

Stow, D., Hope, A., & George, T. (1993). Reflectance characteristics of Arctic Tundra vegetation from aerial radiometry and videography. *International Journal of Remote Sensing*, 14, 1239–1244.

Stow, D. A., Burns, B. H., & Hope, A. S. (1993). Spectral, spatial and temporal characteristics of Arctic tundra reflectance. *International Journal of Remote Sensing*, 14, 2445–2462.

Sturm, M., Racine, C., & Tape, K. (2001). Increasing shrub abundance in the Arctic. *Nature*, 411, 1251–1256.

Suarez, F., Binkley, D., Kaye, M. W., & Stottlemyer, R. (1999). Expansion of forest stands into tundra in the Noatak National Preserve, northwest Alaska. *Ecoscience*, 6, 465–470.

Tahnk, W., & Coakley, J. (2001). Improved calibration coefficients for NOAA-14 AVHRR visible and near-infrared channels. *International Journal of Remote Sensing*, 22, 1269–1284.

Teillet, P. M., & Holben, B. N. (1994). Towards operational radiometric calibration of NOAA AVHRR imagery in the visible and infrared channels. *Canadian Journal of Remote Sensing*, 20(1), 1–10.

Trishchenko, A., Cihlar, J., & Li, Z. (2002). Effects of spectral response function on surface reflectance and NDVI measured with moderate resolution satellite sensors. *Remote Sensing of Environment*, 81, 1–18.

Tucker, C. J. (1979). Red and photographic infrared linear combinations for monitoring vegetation. *Remote Sensing of Environment*, 8, 127–150.

Tucker, C., Slayback, D., Pinzon, J., Los, S., Myneni, R., & Taylor, M. (2001). Higher Northern Latitude NDVI and growing season trends from 1982 to 1999. *International Journal of Biometeorology*, 45, 184–190.

Turner, R. M. (1990). Long-term vegetation change at a fully protected Sonoran desert site. *Ecology*, 71, 464–477.

Vermote, E. E., & El Saleous, N. Z. (1994). Stratospheric aerosol perturbing effect on remote sensing of vegetation: Operational method for the correction of AVHRR composite NDVI. *SPIE Atmospheric Sensing Modelling*, 2311, 19–29.

Vermote, E. F., & Kaufman, Y. J. (1995). Absolute calibration of AVHRR visible and near-infrared channels using ocean and cloud views. *International Journal of Remote Sensing*, 16, 2317–2340.

Viereck, L. A., Dyrness, C. T., Batten, A. R., Wenzlick, K. J. (1992). *The Alaska Vegetation Classification*. General Technical Report, United States Department of Agriculture, Forest Service. Pacific Northwest Research Station.

Vierling, L., Deering, D., & Eck, T. (1997). Differences in Arctic tundra vegetation type and phenology as seen using bidirectional radiometry in he early growing season. *Remote Sensing of Environment*, 60, 71–82.

Vourlitis, G., Oechel, W., Hope, A., Stow, D., Boynton, W., Verfaillie, J. Jr., Zulueta, R., & Hastings, S. (2000). Physiological models for scaling plot measurements of CO_2 flux across an arctic tundra landscape. *Ecological Applications*, 10, 60–72.

Walker, D. A. (1977). *The Analysis of the Effectiveness of a Television Scanning Densiometer for Indicating Geobotanical Features in an Ice Wedge Polygon Complex at Barrow, Alaska*. University of Colorado: Master of Arts Thesis, 132 pp.

Walker, D. A. (1996). Distribution and recovery of Arctic Alaskan vegetation. In J. F. Reynolds, & J. D. Tenhunen (Eds.), *Landscape function and disturbance in Arctic tundra. Ecological Studies*, vol. 120 (pp. 35–71). Heidelberg: Springer.

Walker, D. A., Epstein, H. E., Jia, G. J., Balsar, A., Copass, C., Edwards, E. J., Gould, W. A., Hollingsworth, J., Knudson, J., Meier, H., Moody, A., & Reynolds, M. K. (2003). Phytomass, LAI, and NDVI in northern Alaska: Relationships to summer warmth, soil pH, plant functional types and extrapolation to the circumpolar Arctic. *Journal of Geophysical Research*, 108(D2).

Webber, P. J. (1977). Spatial and temporal variation of the vegetation and its production, Barrow, Alaska. In L. L. Tieszen (Ed.), *The ecology of primary producer organisms in the Alaskan Arctic tundra* (pp. 37–122). New York: Springer.

White, R. G. (1983). Foraging patterns and their multiplier effects on productivity of northern ungulates. *Oikos*, 40, 377–384.

White, R. G., Bunnell, F. L., Gaare, E., Skogland, T., & Hubert, B. (1981). Ungulates on arctic ranges. In L. C. Bliss, O. W. Heal, & J. J. Moore (Eds.), *Tundra ecosystems: A comparative analysis* (pp. 397–483). Cambridge, UK: Cambridge University Press.

White, R. G., & Luick, J. R. (1984). Plasticity and constraints in the

lactational strategy of reindeer and caribou. *Symposium of the Zoological Society of London*, *51*, 215–232.

White, R. G., Thomson, B. R., Skoland, T., Person, S. J., Russell, D. E., Holleman, D. F., & Luick, J. R. (1975). Ecology of caribou at Prudhoe Bay, Alaska. In J. Brown (Ed.), *Ecological investigations of the tundra biome in the Prudhoe Bay region, Alaska. Biological Papers of the University of Alaska. Special Report*, vol. 2 (pp. 151–201).

Williams, M., Eugster, W., Rastetter, E. B., McFadden, J. P., & Chapin III, S. F. (2000). The controls on net ecosystem productivity along an Arctic transect: A model comparison with flux measurements. *Global Change Biology*, *6*(Suppl. 1), 116–126.

Williams, M., & Rastetter, E. B. (1999). Vegetation characteristics and primary productivity along an Arctic transect: Implications for scaling up. *Journal of Ecology*, *87*, 885–898.

Zhou, L., Kaufmann, R. K., Tian, Y., Myneni, R. B., & Tucker, C. J. (2003). Relation between interannual variations in satellite measures of vegetation greenness and climate between 1982 and 1999. *Journal of Geophysical Research*, *108*(D1).

Zhou, L., Tucker, C. J., Kaufmann, R. K., Slayback, D., Shabanov, N. V., & Myneni, R. B. (2001). Variations in northern vegetation activity inferred from satellite data of vegetation index during 1981 to 1999. *Journal of Geophysical Research*, *106*, 20069–20083.